

Received: 2020.08.25

Accepted: 2020.10.04

Available online: 2020.10.21

Published: 2020.12.26

# Laryngeal Squamous Cell Carcinoma: Potential Molecular Mechanism and Prognostic Signature Based on Immune-Related Genes

**Authors' Contribution:**

Study Design A  
Data Collection B  
Statistical Analysis C  
Data Interpretation D  
Manuscript Preparation E  
Literature Search F  
Funds Collection G

**BCEF 1 Bin-Yu Mo\***  
**BCEF 2 Guo-Sheng Li\***  
**DEF 3 Su-Ning Huang**  
**DEF 2 Zhu-Xin Wei**  
**DEF 4 Ya-Si Su**  
**ADG 4 Wen-Bin Dai**  
**ADEG 2 Lin Ruan**

1 Department of Otolaryngology, Liuzhou People's Hospital of Guangxi, Liuzhou, Guangxi, P.R. China  
2 Department of Radiotherapy, First Affiliated Hospital of Guangxi Medical University, Nanning, Guangxi, P.R. China  
3 Department of Radiotherapy, Guangxi Medical University Cancer Hospital, Nanning, Guangxi, P.R. China  
4 Department of Pathology, Liuzhou People's Hospital, Liuzhou, Guangxi, P.R. China

\* Bin-Yu Mo and Guo-Sheng Li contributed equally to this work and are considered to be co-first authors

**Corresponding Authors:**

**Source of support:**

Wen-Bin Dai, e-mail: [daiwenbin1973@163.com](mailto:daiwenbin1973@163.com), Lin Ruan, e-mail: [ruan\\_lin\\_gxmuyfy@163.com](mailto:ruan_lin_gxmuyfy@163.com)

The study was supported by funding from the National Natural Science Foundation of China (81460479)

**Background:**

Immune-related genes (IRGs) are closely related to the incidence and progression of tumors, potentially indicating that IRGs play an important role in laryngeal squamous cell carcinoma (LSCC).

**Material/Methods:**

An RNA sequencing dataset containing 123 samples was collected from The Cancer Genome Atlas. Based on immune-related differentially expressed genes (IRDEGs), a potential molecular mechanism of LSCC was explored through analysis of information in the Gene Ontology (GO) resource and the Kyoto Encyclopedia of Genes and Genomes (KEGG), and protein-protein interactions (PPIs). A regulatory network of transcriptional regulators and IRDEGs was constructed to explore the underlying molecular mechanism of LSCC at the upstream level. Candidates from IRDEGs for signature were screened via univariate Cox analysis and using the least absolute shrinkage and selection operator (LASSO) technique. The IRDEG signature of LSCC was constructed by using a multivariate Cox proportional hazards model.

**Results:**

GO and KEGG analysis showed that IRDEGs may participate in the progression of LSCC through immune-related reactions. PPI analysis demonstrated that, among the IRDEGs in LSCC, the Kininogen 1; C-X-X motif chemokine ligand 10; elastase, neutrophil expressed; and *LYZ* genes are hub genes in the development of LSCC. At the upstream level, *SP11*, *SP140*, signal transducer and activator of transcription 4, zinc finger E-box binding homeobox, and Ikaros family zinc finger 2 are the hub transcriptional regulators of IRDEGs. The risk score based on the IRDEG signature was able to distinguish prognosis in patients with LSCC and represents an independent prognostic risk factor for LSCC.

**Conclusions:**


From the perspective of IRGs, we first constructed an IRDEG signature related to the prognosis of LSCC, which can be used as a novel marker to predict prognosis in patients with LSCC.

**MeSH Keywords:**

**Carcinoma, Squamous Cell • Databases, Nucleic Acid • Immunity • Prognosis • Transcriptome**

**Full-text PDF:**

<https://www.medscimonit.com/abstract/index/idArt/928185>

 4155

 3

 16

 62



## Background

Laryngeal squamous cell carcinoma (LSCC) is currently the most common pathological classification of laryngeal carcinoma (LC), accounting for more than 90% of cases [1–6]. Globally, more than 177 000 cases of LC are diagnosed every year, and more than 94 000 deaths from the disease [7]. Currently, treatments such as surgery, radiation therapy, and chemotherapy are used for early-stage LC [8,9], with favorable effects on survival [10–12]. However, more than two-thirds of patients are diagnosed with LC when the disease is already at an advanced stage [13–16]. This delay facilitates the growth and spread of LC cells [17], posing challenges for successful treatment of the disease.

Several pathogenic factors and mechanisms have been proposed for LC. Previous research has found that the incidence and development of it may be related to multiple risk factors, such as drinking [18–20], smoking [13], asbestos exposure [21], and human papillomavirus infection [22]. The mechanism may involve multiple molecules (such as MYC Target 1 [23], *p16* [24], and *NLK* [25]), and multiple pathways (such as Wnt/ $\beta$ -catenin [26], ATR/*p53*/caspase-3 [27], and phosphatidylinositol-3-kinase/Akt/mTOR [28]); clearly, the onset and development of LC are complex. In summary, it is necessary to further explore the molecular mechanism of the pathogenesis and development of LC and identify novel and effective prognostic markers to assist in clinical screening and treatment of LC.

The immune system has been considered to affect the development, growth, and metastasis of tumors. Immune-related genes (IRGs) are considered to be relevant to tumor prognosis. For example, high expression of *FGF19* may promote breast cancer progression by activating Akt signaling in cells, resulting in a discouraging prognosis for individuals with the disease [29]. Similarly, in esophageal squamous cell carcinoma, patients with *TUBB3*-negative carcinomas had higher rates of disease-free survival (DFS) and overall survival (OS) rates than those with *TUBB3*-positive disease [30]. In glioblastomas, another IRG, *RBP1*, is considered to be associated with poor prognosis [31]. Studies of LSCC and IRGs have found that programmed death-ligand 1 (PD-L1) expression is associated with favorable prognosis [32], and *STC2* [33] overexpression is associated with poor prognosis. Clearly, IRGs are likely to contribute to the incidence, growth, and spread of LSCC. Therefore, exploring the relationship between IRGs and LSCC prognosis is crucial to understanding the pathogenesis of the disease and facilitating clinical screening and treatment.

High-throughput sequencing technologies are widely used in cancer multi-omics. In this study, we combined high-throughput data from public databases and published studies to explore the potential molecular mechanism of development of

LSCC and to identify a prognostic signature based on IRGs to assist in clinical screening and treatment of LSCC.

## Material and Methods

### Collection of sample data and IRGs

The RNA sequencing (RNA-Seq) dataset from The Cancer Genome Atlas (TCGA) was obtained through the Genomic Data Commons Data Portal database (<https://portal.gdc.cancer.gov/repository>). The dataset contained 111 LSCC samples and 12 non-LSCC control samples. Clinical information from the samples in the RNA-Seq dataset was obtained from the University of California Santa Cruz Xena database (<http://xena.ucsc.edu/>). In addition, a list of 1811 IRGs was obtained from the ImmPort database (<https://www.immport.org/home>).

### Differential expression analysis

RNA-Seq count data were input into R (v3.6.1), and through the edgeR package [34], differentially expressed genes (DEGs) that had a  $\log_2$ -fold change of 2 or more and an adjusted  $P < 0.05$  were selected for further study. Genes were identified as up-regulated (up-DEGs) if they showed a  $\log_2$ -fold change of 2 or more, while genes with a  $\log_2$  fold change less than  $-2$  were considered downregulated (down-DEGs). The same methods were used to screen immune-related differentially expressed genes (IRDEGs), immune-related upregulated DEGs (up-IRDEGs), and immune-related downregulated DEGs (down-IRDEGs).

### Analysis of the potential molecular mechanism of IRDEGs

Gene Ontology (GO) and Kyoto Encyclopedia of Genes and Genomes (KEGG) pathway enrichment analyses of up-IRDEGs and down-IRDEGs were performed using the clusterProfiler package [35] in R (v3.6.1). GO terms and KEGG signaling pathways were then filtered by identifying those that simultaneously satisfied the following 3 conditions: (1) adjusted  $P < 0.05$ ; (2)  $q < 0.05$ ; and (3) number of enriched genes  $\geq 5$ . The STRING database (<https://string-db.org/>) was used for analysis of protein-protein interactions (PPIs) of up-IRDEGs and down-IRDEGs. The minimum required interaction score for a PPI was set at 0.7 in the STRING database, which is considered by the database as high confidence. The CytoHub plug-in in Cytoscape software (v3.7.2) was applied to screen for hub genes, and the hub genes of up-IRDEGs and down-IRDEGs were identified according to the degree algorithm.

### Transcriptional regulator (TR) prediction for IRDEGs and construction of TR-mediated regulatory network

To further understand the potential molecular mechanisms of up-IRDEGs and down-IRDEGs in LSCC, we attempted to explore

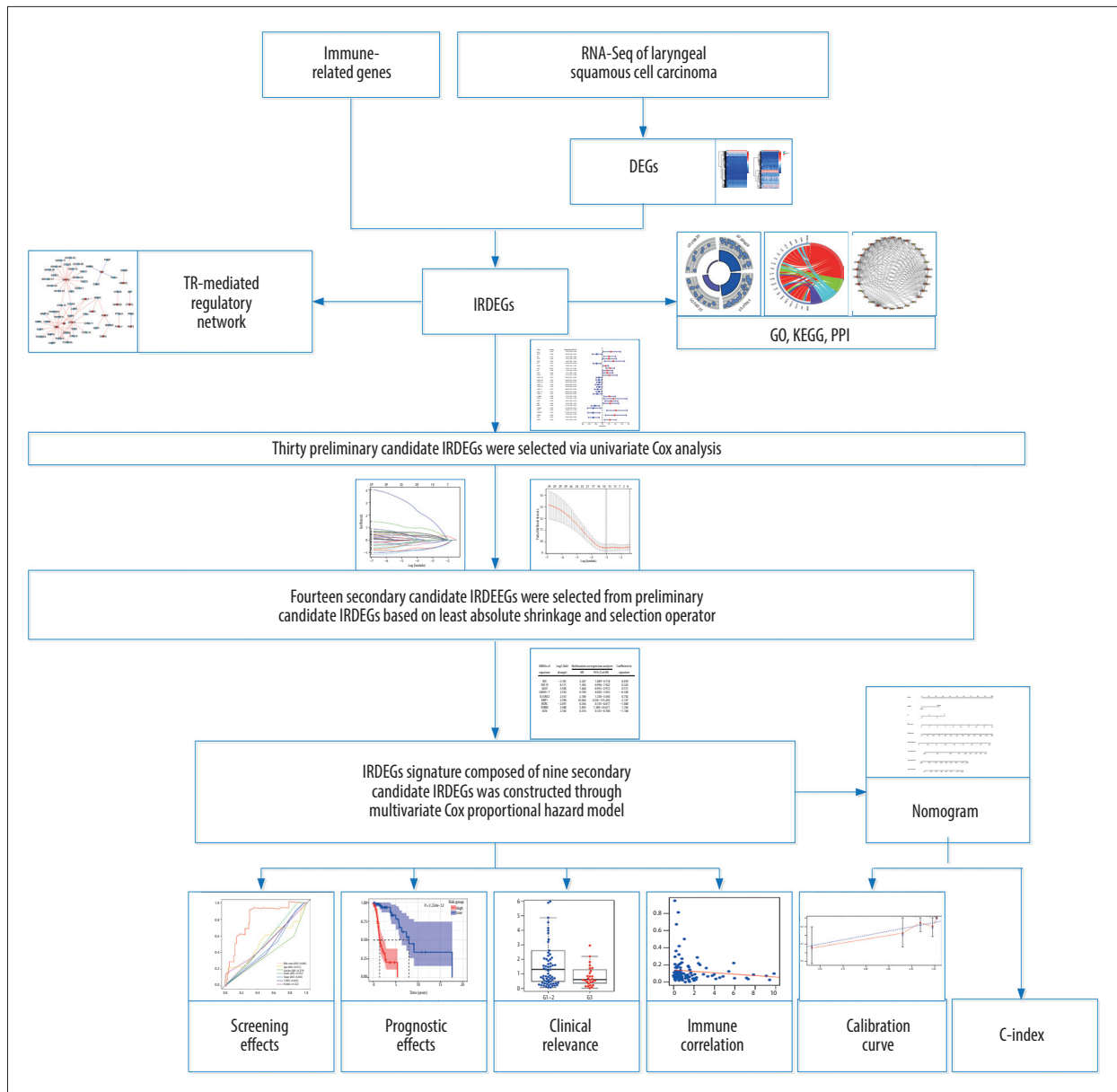


**Figure 1.** The main processes of this study. DEGs – differentially expressed genes; IRDEGs – immune-related differentially expressed genes; GO – Gene Ontology; KEGG – Kyoto Encyclopedia of Genes and Genomes; PPI – protein–protein interaction; TR – transcriptional regulator; C-index – concordance index.

the upstream regulation mechanism of these genes through the correlation between the genes and transcriptional regulators (TRs). TRs for genes were predicted using Epigenetic Landscape In Silico (Lisa, <http://lisa.cistrome.org/>), a bioinformatics analysis tool [36] that contains a large amount of H3K27ac ChIP-seq data from Homo sapiens. We predicted TRs related to up-IRDEGs and down-IRDEGs with the Lisa tool and selected TRs with  $P < 0.01$ . Pearson coefficients of expression levels of TRs and IRDEGs were calculated in R, while the TR-IRDEG regulatory network was constructed using Cytoscape.

### Development and assessment of IRDEG signature

Univariate Cox analysis and least absolute shrinkage and selection operator (LASSO) were used to select the candidates for signature from IRDEGs, and a multivariate Cox proportional hazards model was applied to construct the IRDEG signature of LSCC based on candidate IRDEGs (Figure 1). Using univariate Cox analysis, IRDEGs related to the survival of patients with LSCC ( $P < 0.05$ ) were identified and named as preliminary candidate IRDEGs. Then, based on the LASSO regression analysis, which can quickly and effectively extract important variables

from many variables, secondary candidate IRDEGs were obtained from the preliminary candidate IRDEGs. Eventually, through the multivariate Cox proportional hazard model, some of the secondary candidate IRDEGs were used to construct the IRDEG signature of LSCC.

Curves for receiver operating characteristics (ROCs) and survival analysis (Kaplan-Meier) were used to evaluate the relationship between the IRDEG signature and the effects on screening and prognosis, respectively. Univariate and multivariate Cox regression analyses were used to identify factors related to independent prognoses in the IRDEG signature and clinical parameters. Development and assessment of the IRDEG signature were completed in R with the help of the glmnet [37], survival, and survivalROC package [38].

### Relationship between risk score of IRDEG signature and immune infiltration level

The Tumor IMmune Estimation Resource (TIMER, <https://cistrome.shinyapps.io/timer/>) is an online tool for comprehensive analysis of tumor infiltration of immune cells. The table matrix of TCGA estimation in TIMER was used to analyze the correlation between the IRDEG signature infiltration level risk score and 6 types of immune cells: B cells, CD4 T cells, CD8 T cells, macrophages, neutrophils, and dendritic cells.

### Application of IRDEG signature

Combining the IRDEG signature and the clinical parameters related to the independent prognosis of LSCC, a nomogram was constructed to quantify the risk of LSCC in individuals in a clinical environment. A calibration curve was used to detect the difference between the predicted and actual survival rates in the nomogram. The concordance index (C-index; range 0–1) was used to objectively evaluate the predictive power of the signature; the larger the C-index, the better the predictive power of the signature. Construction and verification of the nomogram were performed in R.

### Statistical analysis

Except for differential expression analysis, for which original counts should be used, the RNA-Seq data used in the rest of the analysis were  $\log_2(\text{counts}+1)$  converted data. All statistical analyses were performed in R.

The main processes in the present study are shown in Figure 1. Unless otherwise specified,  $P < 0.05$  for a difference was considered statistically significant.

## Results

### Identification of DEGs and IRDEGs in LSCC

After filtering, 4274 DEGs were included: 2990 up-DEGs and 1284 down-DEGs. Among the 1811 IRGs, there were 302 IRDEGs, including 224 up-IRDEGs and 78 down-IRDEGs. Supplementary Figure 1 shows the expression of DEGs and IRDEGs in LSCC.

### GO, KEGG, and PPI analyses of IRDEGs

To analyze the potential molecular mechanism of LSCC, we conducted GO, KEGG, and PPI analyses of IRDEGs.

GO analysis was performed on 224 up-IRDEGs and 78 down-IRDEGs. Among up-IRDEGs, the most common biological terms were “complement activation, classical pathway” (“biological process”), “blood microparticle” (“cell component”), and “antigen binding” (“molecular function”) (Figure 2A–2C). For down-IRDEGs, the most common biological process, cell component, and molecular function terms were “antimicrobial humoral response,” “azurophil granule lumen,” and “receptor ligand activity,” respectively (Supplementary Figure 2A–2C). Table 1 shows the 4 most enriched terms among the 3 types of terms.

KEGG analysis results showed that the most enriched KEGG pathway for both up-IRDEGs (Figure 3) and down-IRDEGs (Supplementary Figure 3) was the “cytokine-cytokine receptor interaction.” The 4 most enriched pathways for up-IRDEGs and down-IRDEGs are shown in Figure 3, Supplementary Figure 3, and Table 1. The GO and KEGG analyses show that the biological terms enriched in IRDEGs and the KEGG signaling pathway are closely related to immunity. In fact, these results are not surprising, given that the IRDEGs used for KEGG analysis were originally genes closely related to immunity.

The results of the PPI analysis and the degree algorithm showed that in up-IRDEGs, Kininogen 1 (*KNG1*) and C-X-C motif chemokine ligand 10 (*CXCL10*) were hub genes in the development of LSCC, while in down-IRDEGs, the hub genes were elastase, neutrophil expressed (*ELANE*) and lysozyme (*LYZ*). Figure 4A and 4B, respectively, show the interaction between the first 30 up-IRDEGs and down-IRDEGs obtained with the Degree algorithm.

### Construction of a TR-mediated regulatory network

Based on the prediction results from the Lisa tool, we screened 103 up-TRs related to up-IRDEGs with a threshold of  $P < 0.01$ . To reduce false positives in TR prediction results, we conducted a correlation analysis on the 96 up-TRs included in up-IRDEGs and RNA-Seq and finally selected 15 real up-TRs and 50 up-IRDEGs with Pearson correlation coefficients  $> 0.5$  and

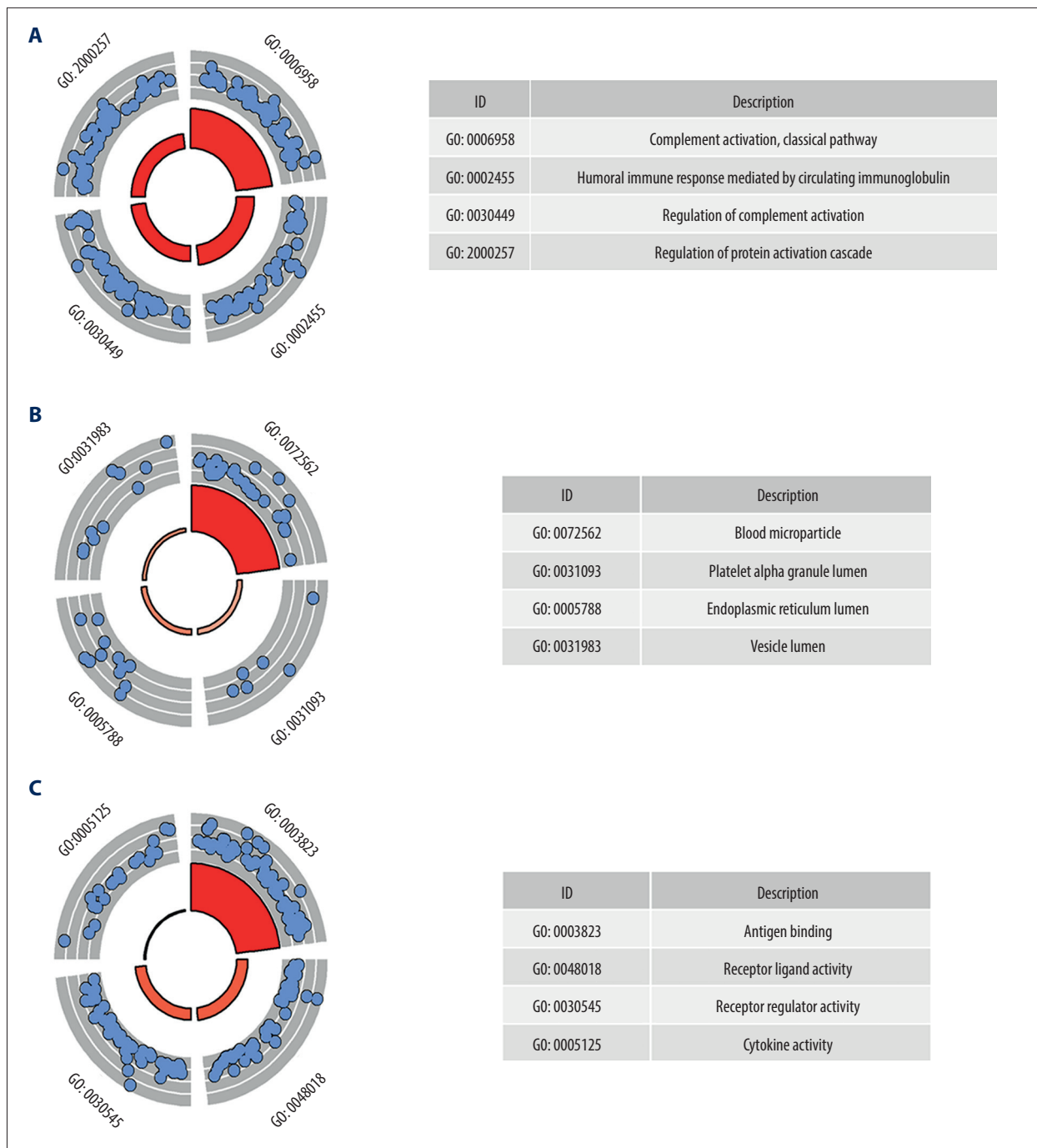


**Figure 2.** Gene Ontology (GO) analysis for immune-related upregulated differentially expressed genes. **(A)** Biological process. **(B)** Cellular component. **(C)** Molecular function. The blue nodes in the concentric circles represent genes clustered in specific GO terms. The larger size and darker color of the internal departments represent more significant enrichment of GO terms.

**Table 1.** Gene Ontology analysis (GO) and Kyoto Encyclopedia of Genes and Genomes (KEGG) analysis for immune-related up-regulated differentially genes and immune-related down-regulated differentially genes.

Category	ID	Description	P. adjust	Q value	Count
GO-BP	GO: 0006958	Complement activation, classical pathway	3.57E-65	2.95E-65	46
GO-BP	GO: 0002455	Humoral immune response mediated by circulating immunoglobulin	6.27E-62	5.17E-62	46
GO-BP	GO: 0030449	Regulation of complement activation	2.89E-61	2.38E-61	47
GO-BP	GO: 2000257	Regulation of protein activation cascade	3.59E-61	2.96E-61	47
GO-CC	GO: 0072562	Blood microparticle	3.93E-29	3.70E-29	30
GO-CC	GO: 0031093	Platelet alpha granule lumen	0.002598	0.002448	6
GO-CC	GO: 0005788	Endoplasmic reticulum lumen	0.002598	0.002448	12
GO-CC	GO: 0031983	Vesicle lumen	0.036346	0.034244	10
GO-MF	GO: 0003823	Antigen binding	2.12E-88	1.81E-88	64
GO-MF	GO: 0048018	Receptor ligand activity	2.65E-32	2.27E-32	45
GO-MF	GO: 0030545	Receptor regulator activity	3.66E-31	3.13E-31	45
GO-MF	GO: 0005125	Cytokine activity	5.77E-15	4.93E-15	20
KEGG	hsa04060	Cytokine-cytokine receptor interaction	2.32E-22	2.09E-22	33
KEGG	hsa04061	Viral protein interaction with cytokine and cytokine receptor	2.47E-11	2.23E-11	15
KEGG	hsa04062	Chemokine signaling pathway	1.47E-06	1.33E-06	14
KEGG	hsa04080	Neuroactive ligand-receptor interaction	1.88E-06	1.69E-06	18
GO-BP	GO: 0019730	Antimicrobial humoral response	4.50E-08	3.61E-08	10
GO-BP	GO: 0006959	Humoral immune response	2.16E-05	1.74E-05	11
GO-BP	GO: 0009620	Response to fungus	3.92E-05	3.14E-05	6
GO-BP	GO: 0031640	Killing of cells of other organism	6.00E-05	4.82E-05	6
GO-CC	GO: 0035578	Azurophil granule lumen	1.25E-05	1.06E-05	7
GO-CC	GO: 0005775	Vacuolar lumen	3.27E-05	2.76E-05	8
GO-CC	GO: 0031983	Vesicle lumen	3.27E-05	2.76E-05	10
GO-CC	GO: 0031012	Extracellular matrix	0.000352	0.000297	10
GO-MF	GO: 0048018	Receptor ligand activity	1.81E-24	1.40E-24	28
GO-MF	GO: 0030545	Receptor regulator activity	6.03E-24	4.65E-24	28
GO-MF	GO: 0005125	Cytokine activity	1.04E-14	8.01E-15	15
GO-MF	GO: 0008201	Heparin binding	1.07E-05	8.23E-06	8
KEGG	hsa04060	Cytokine-cytokine receptor interaction	2.88E-12	2.72E-12	19
KEGG	hsa04659	Th17 cell differentiation	0.02884	0.02727	5
KEGG	hsa04630	JAK-STAT signaling pathway	0.02884	0.02727	6
KEGG	hsa05321	Inflammatory bowel disease (IBD)	0.02884	0.02727	4

Count – count of genes enriched in the category; BP – biological process; CC – cellular component; MF – molecular function. The deep blue area was based on the analysis of immune-related up-regulated differentially genes while the light blue area was based on the analysis of immune-related down-regulated differentially genes.

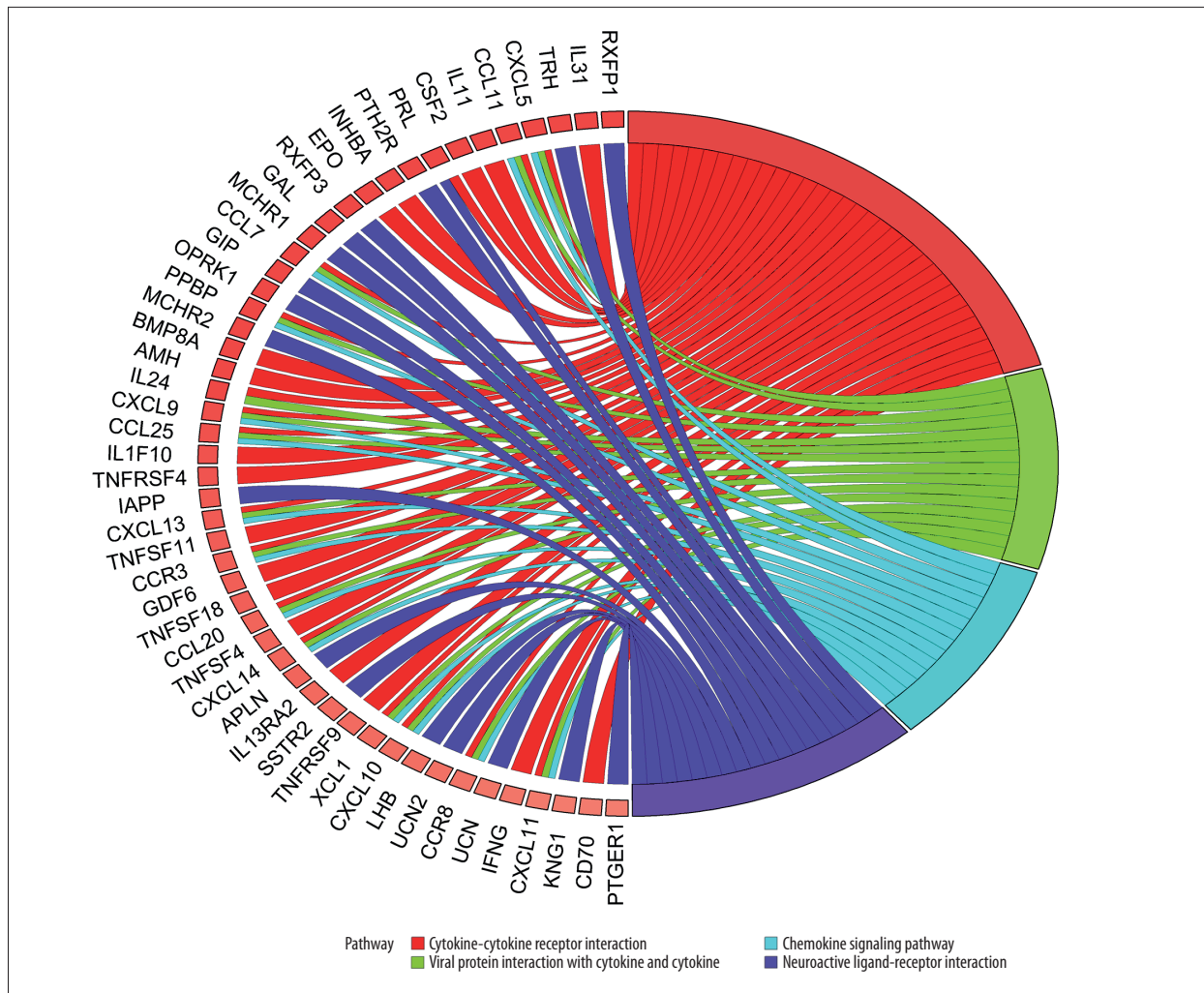


**Figure 3.** Kyoto Encyclopedia of Genes and Genomes (KEGG) analysis of immune-related upregulated differentially expressed genes. Different color bands correspond to different KEGG enrichment pathways.

$P < 0.05$  for constructing up-TR-IRDEGs. The results showed that *SPI1*, *SPI140*, and signal transducer and activator of transcription 4 (*STAT4*) were likely to be the hub TRs regulating up-IRDEGs (Figure 5A).

In the same way, we screened 159 down-TRs, 147 of which were included in the RNA-Seq dataset used in this study. Finally, we selected 17 real down-TRs and 24 down-IRDEGs with correlation coefficients  $> 0.5$  to construct down-TRs-IRDEGs. The results indicated that zinc finger E-box binding homeobox (*ZEB1*) and Ikaros family zinc finger 2 (*IKZF2*) may be important TRs in regulating down-IRDEGs (Figure 5B).

### Construction of IRDEGs signature

Through univariate Cox analysis, 30 preliminary candidate IRDEGs related to the survival of patients with LSCC were obtained from 302 IRDEGs, as shown in Supplementary Figure 4.

Based on LASSO regression analysis and selecting the largest lambda with an average error within 1 standard deviation, 14 secondary candidate IRDEGs for construction of an IRDEG signature were selected from as many as 30 preliminary IRDEGs (Supplementary Figure 5). In total, 14 secondary candidate IRDEGs – beta cellulin (*BTC*), *EPO*, fibroblast growth factor (*FGF*)19, *FGF5*, gastrin (*GAST*), immunoglobulin heavy chain variable (*IGHV*)3–7, *IGHV6–1*, interleukin 13 receptor subunit alpha 2 (*IL13RA2*, retinol binding protein 1 (*RBP1*), RAR related orphan receptor C (*RORC*), semaphoring 6C (*SEMA6C*), TNFR receptor superfamily member 4 (*TNFRSF4*), *TUBB3*, and urocortin (*UCN*) – were used to construct the IRDEG signature. Finally, we used the multivariate Cox proportional hazards model to construct the IRDEG signature of LSCC. The final IRDEG signature contained 9 secondary candidate IRDEGs for LSCC. As shown in Table 2, of the 9 IRDEGs, 7 (*FGF19*, *GAST*, *IGHV3–7*, *IL13RA2*, *RBP1*, *TUBB3*, *UCN*) were highly expressed in LSCC, while *IL13RA2*, *RBP1*, and *TUBB3* are prognostic risk factors for

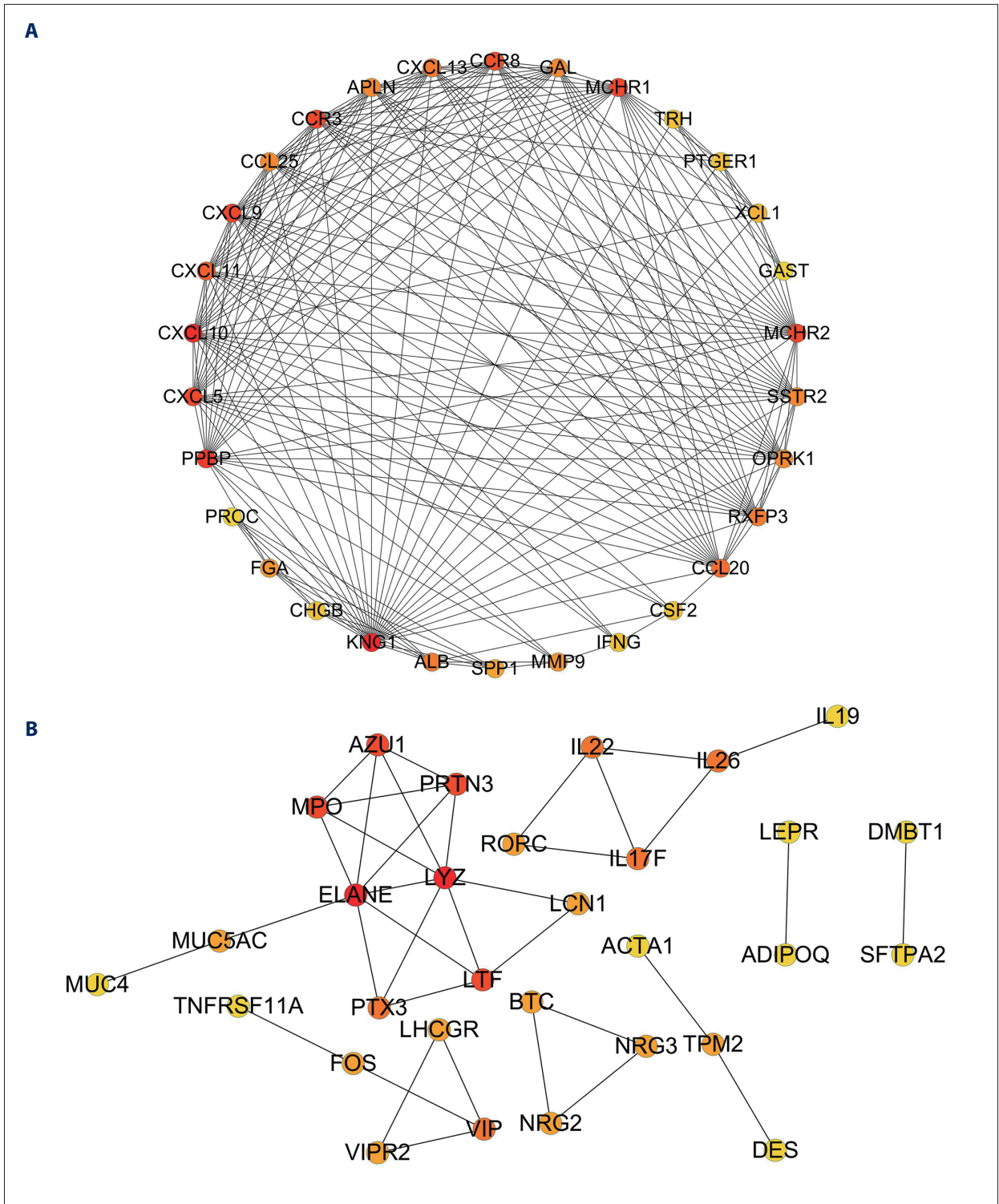


**Figure 4.** Protein-protein interaction analysis. **(A)** Immune-related upregulated differentially expressed genes. **(B)** Immune-related downregulated differentially expressed genes.



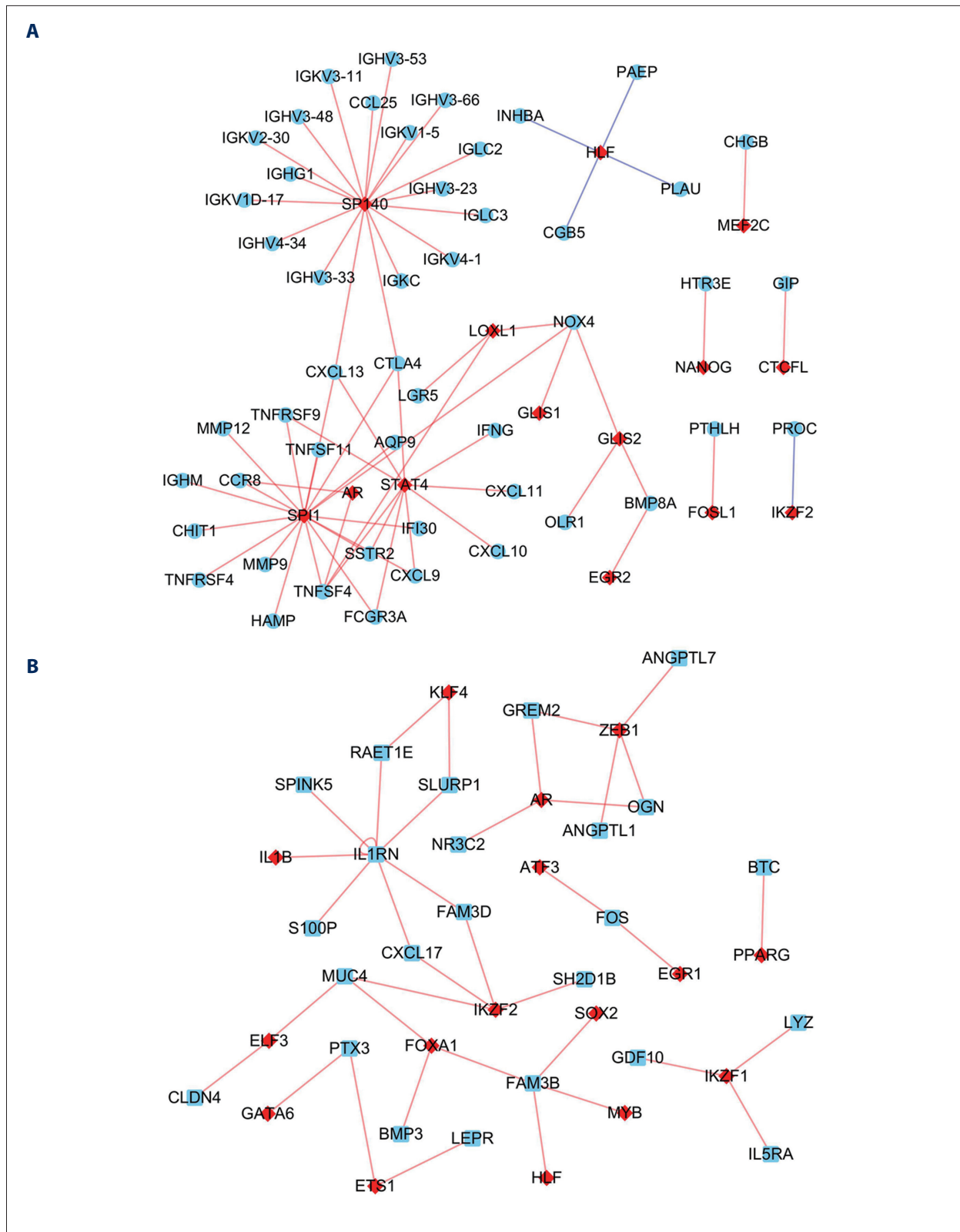


**Figure 5.** Transcriptional regulator (TR)-mediated regulatory networks. **(A)** Immune-related upregulated differentially expressed genes. **(B)** Immune-related downregulated differentially expressed genes. The red and blue nodes represent TRs and immune-related differentially expressed genes, respectively. The red and blue edges represent positive and negative correlation, respectively.

**Table 2.** Immune-related differentially expressed genes (IRDEGs) included in the signature.

IRDEGs of signature	Log <sub>2</sub> (fold change)	Multivariate Cox regression analyses		Coefficient in signature
		HR	95% CI of HR	
BTC	-2.181	2.267	1.089-4.718	0.818
FGF19	8.111	1.383	0.996-1.922	0.325
GAST	5.928	1.668	0.955-2.912	0.511
IGHV3-7	2.533	0.720	0.502-1.033	-0.328
IL13RA2	2.413	2.100	1.230-3.584	0.742
RBP1	2.596	23.026	3.416-155.202	3.137
RORC	-2.691	0.344	0.145-0.817	-1.068
TUBB3	2.400	5.835	1.380-24.671	1.764
UCN	2.183	0.314	0.141-0.700	-1.160

HR – hazard ratio; CI – confidence interval.

patients with LSCC (hazard ratio [HR] >1 and 95% confidence interval [CI] do not contain 1). Of the 9 IRDEGs, *BTC* and *RORC* are expressed at low levels in LSCC and *BTC* is a risk factor for patients with LSCC, while *RORC* is a prognostic protective factor (HR <1 and 95% CI do not contain 1). The 9 genes included in the IRDEG signature as well as the coefficients of each gene are listed in Table 2. The product of the expression value of each gene and the gene's corresponding coefficient is the contribution of the gene to the risk score, and the sum of the contribution of all genes is the risk score, and we performed a risk score calculation for 111 LSCC samples.

### Validation of IRDEG signature

To evaluate the screening and prognostic effects of the signature in LSCC prognosis, patients with LSCC were divided into high- and low-risk groups according to scores higher or lower than the median risk score (0.859).

In terms of screening, the ROC curve showed that the risk score calculated according to the signature was the best measure for determining the survival of patients with LSCC, with a higher area under the curve than any clinical parameter (age, sex, neoplasm histologic grade, stage, tumor stage, node stage; Figure 6A) and any single gene included in the IRDEG signature (Figure 6B). Moreover, we also compared the performance of the signature to potential markers related to the prognosis of LSCC identified in research recently added to PubMed (published between January 1, 2020 and May 15, 2020), while 9 of the potential markers – activated leukocyte cell adhesion molecular (*ALCAM*) [39], *ATM* [40], BAF chromatin remodeling complex subunit (*BCL11A*) [41], B-cell lymphoma 2 (*BCL-2*) [42], desmoglein 2 (*DSG2*) [43], epidermal growth factor receptor

(*EGFR*) [44], *FGFR1* [45], homeobox A13 (*HOXA13*) [46], insulin like growth factor 1 receptor (*IGF-1R*) [47] – were included in the RNA-Seq data used in this study. Compared with any gene from these 9 potential prognostic markers, the risk score based on the IRDEG signature showed the best ability to screen for prognosis in patients with LSCC (Figure 6C).

In terms of prognosis, the OS rate for the high-risk group was significantly lower than that for the low-risk group (Figure 6D,  $P=1.234e-12$ ). Moreover, the risk curve showed that the majority of patients with LSCC who died were those with a higher risk score, whereas there were significantly fewer deaths in the group with low-risk scores (Figure 7A). Figure 7B shows the expression of the 9 IRDEGs in the signature in the high- and low-risk groups.

In addition, we used Cox regression analysis to explore prognostic factors in LSCC. The results of univariate and multivariate Cox regression analysis demonstrated that the risk score based on the IRDEG signature can be considered a risk factor for the independent prognosis of LSCC (Figure 8A, 8B). In terms of risk of death, the risk for men with LSCC was 0.432 times that for women, whereas the node stage of the tumor was a risk factor related to the prognosis of LSCC (Figure 8B).

### Relationship between IRDEG signature and clinical parameters in patients with LSCC

To explore the clinical significance of IRDEGs in the signature of LSCC, we studied the expression of each IRDEG in the signature and its relationship with clinical parameters. Among the 9 IRDEGs included in the signature, *BTC* and *RORC* had low levels of expression in LSCC and the remaining 7 genes were

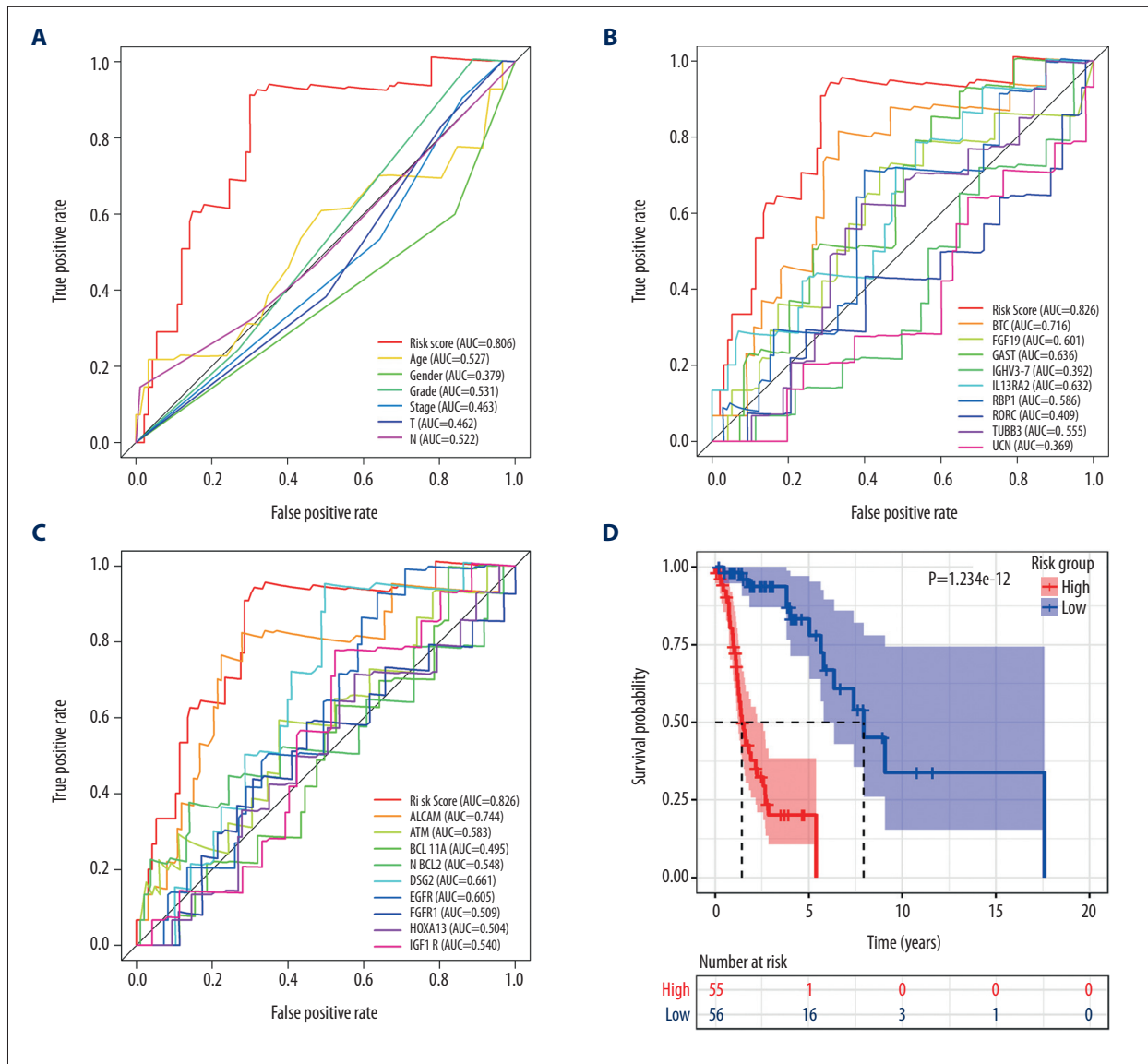


**Figure 6.** Signature of immune-related differentially expressed genes (IRDEGs). Receiver operating characteristic curves. (A) Risk score and clinical parameters. (B) IRDEGs. (C) Nine prognostic markers. (D) Kaplan-Meier curve of high- and low-risk groups, which were classified based on median risk score of IRDEGs signature.

highly expressed in LSCC. A Wilcoxon test showed that there were statistically significant differences in expression of 6 of the remaining 7 genes in the LSCC and non-LSCC samples. The exception was *IL13RA2* (Figure 9A). Subsequently, based on data from 102 patients with LSCC for whom we had complete clinical information (Supplementary Table 1), we explored the relationship between risk score and expression level of the 9 genes and the clinical parameters in the patients (age, sex, neoplasm histologic grade, stage, and tumor and node stage), and found that the risk score and *GAST* were related to the neoplasm histologic grade of LSCC (Figure 9B, 9C), while the levels of expression of *BTC*, *RORC*, and *TUBB3* were related to the age of patients with LSCC (Figure 9D–9F).

In addition, we analyzed the relationship between the IRDEG signature and the infiltration levels of B and CD4 and CD8 T cells; macrophages; neutrophils; and dendritic cells and found that the risk score based on the IRDEG signature was negatively correlated with the level of B-cell immune infiltration (Supplementary Figure 6).

### Construction and verification of nomogram based on IRDEG signature

To investigate a preliminary application of the IRDEG signature, we constructed a nomogram of it and the clinical parameters

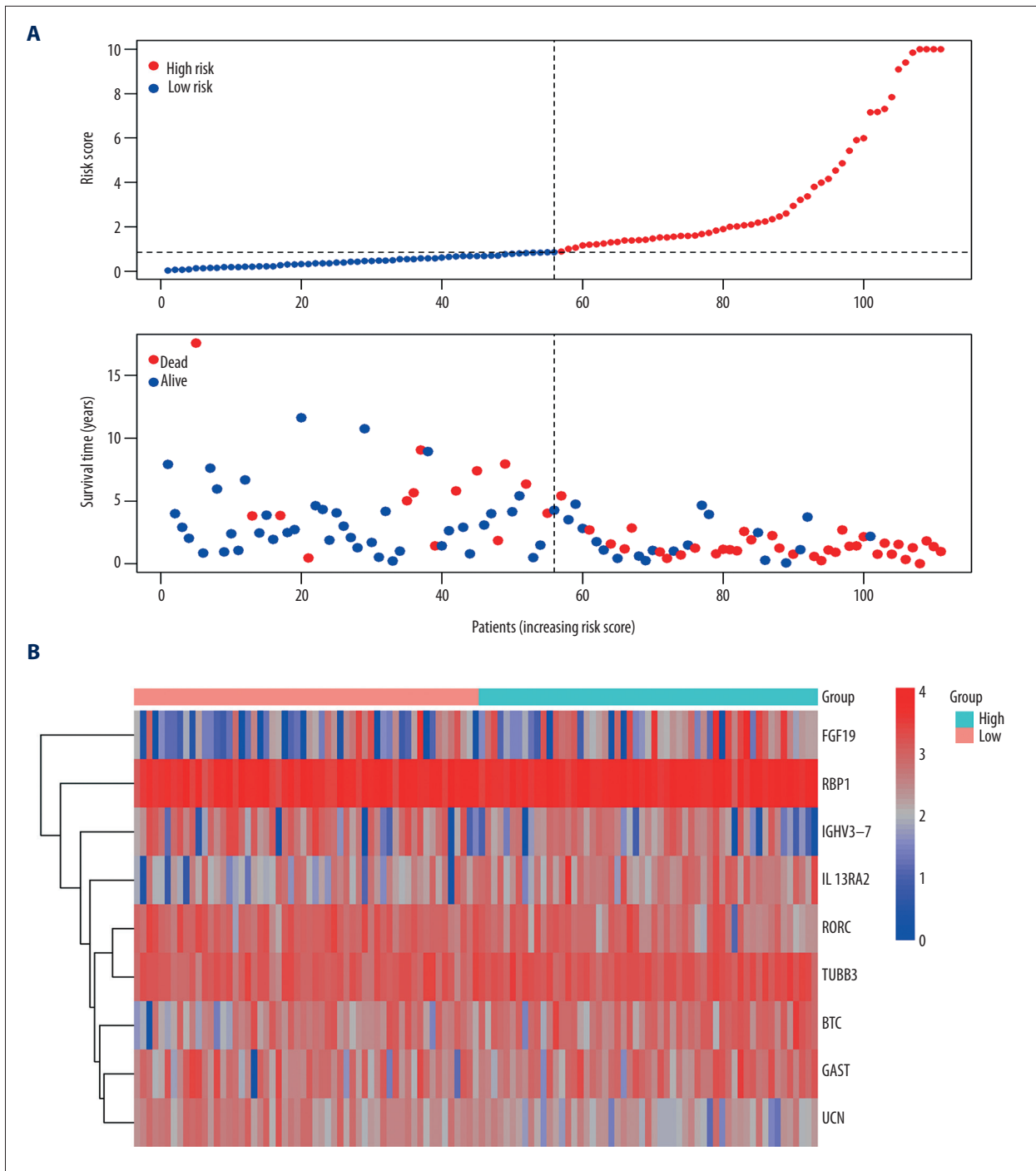


**Figure 7.** (A) Risk plots for high- and low-risk groups. Each blue dot represents a living patient, whereas each red dot represents a dead patient. (B) Heatmap of expression levels of the 9 genes in response to IRDEGs signature in patients.

related to independent prognosis of LSCC and predicted 1-, 3-, and 5-year survival rates in patients with LSCC (Figure 10A).

The calibration curve revealed that although the 3- and 5-year survival rate predictions by the nomogram were not in good agreement with actual patient survival (data not shown), the

1-year survival rate predictions were close to actual survival (Figure 10B). Moreover, the more objective C-index was 0.777 (standard deviation=0.031), indicating that the nomogram could predict the survival rate with moderate accuracy.

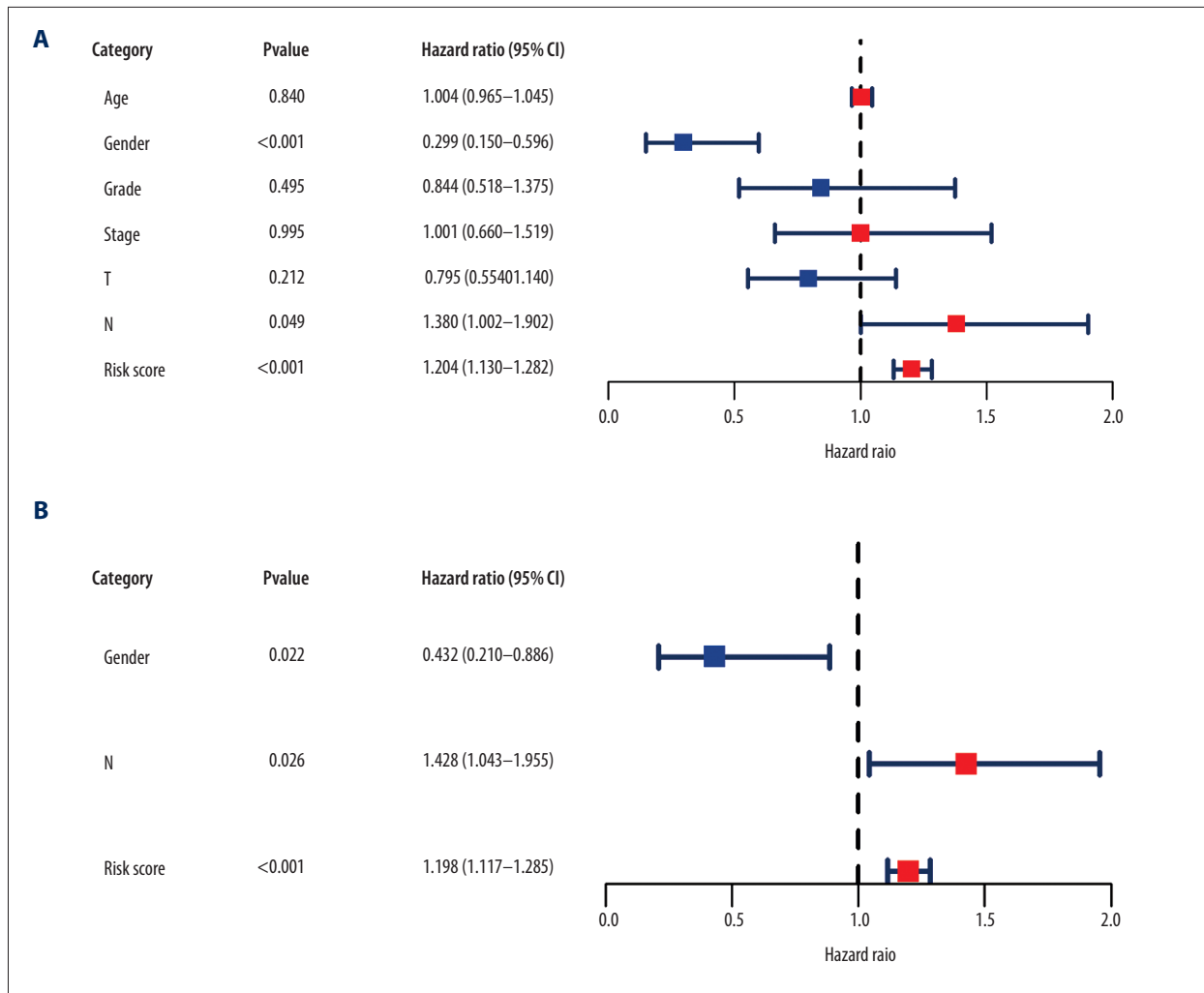


**Figure 8.** Forest plots reflecting factors related to independent prognosis of laryngeal squamous cell carcinoma. (A) Plot based on univariate Cox regression analysis. (B) Plot based on multivariate Cox regression analysis.

## Discussion

According to current research, a number of IRGs are closely related to the incidence and progression of tumors, potentially indicating that IRGs play an important role in cancer [32]. Therefore, new markers for screening and treatment of tumors could be discovered through exploration of and research about IRGs.

Using the RNA-Seq dataset containing 123 samples, we first explored the potential molecular mechanism of LSCC from the perspective of IRGs, and for the first time, constructed an IRDEG signature related to the prognosis of LSCC based on IRGs. Through GO and KEGG analysis, we found, as expected, that IRDEGs may participate in the progression of LSCC through immune-related reactions. PPI analysis identified hub genes among IRDEGs in LSCC. We then constructed a regulatory network of TRs and IRDEGs to explore the underlying molecular

mechanism of LSCC at the upstream level. In addition, the risk score based on the IRDEG signature that we constructed did well in distinguishing the prognosis of patients with LSCC. The risk score based on the IRDEG signature was an independent prognostic risk factor for LSCC, indicating that the IRDEG signature can be used as a novel marker to predict prognosis in patients with LSCC.

Initially, we explored the underlying molecular mechanism of LSCC from the perspective of IRGs. To this end, we conducted enrichment and PPI analyses on IRDEGs. In up-IRDEGs, the most common GO terms in biological processes, cellular components, and molecular functions were “complement activation, classical pathway,” “blood microparticle,” and “antigen binding,” respectively, while in down-IRDEGs, the terms were “antimicrobial humoral response,” “azurophil granule lumen,” and “receptor ligand activity,” respectively. The KEGG analysis revealed that the most enriched pathways for both up-IRDEGs

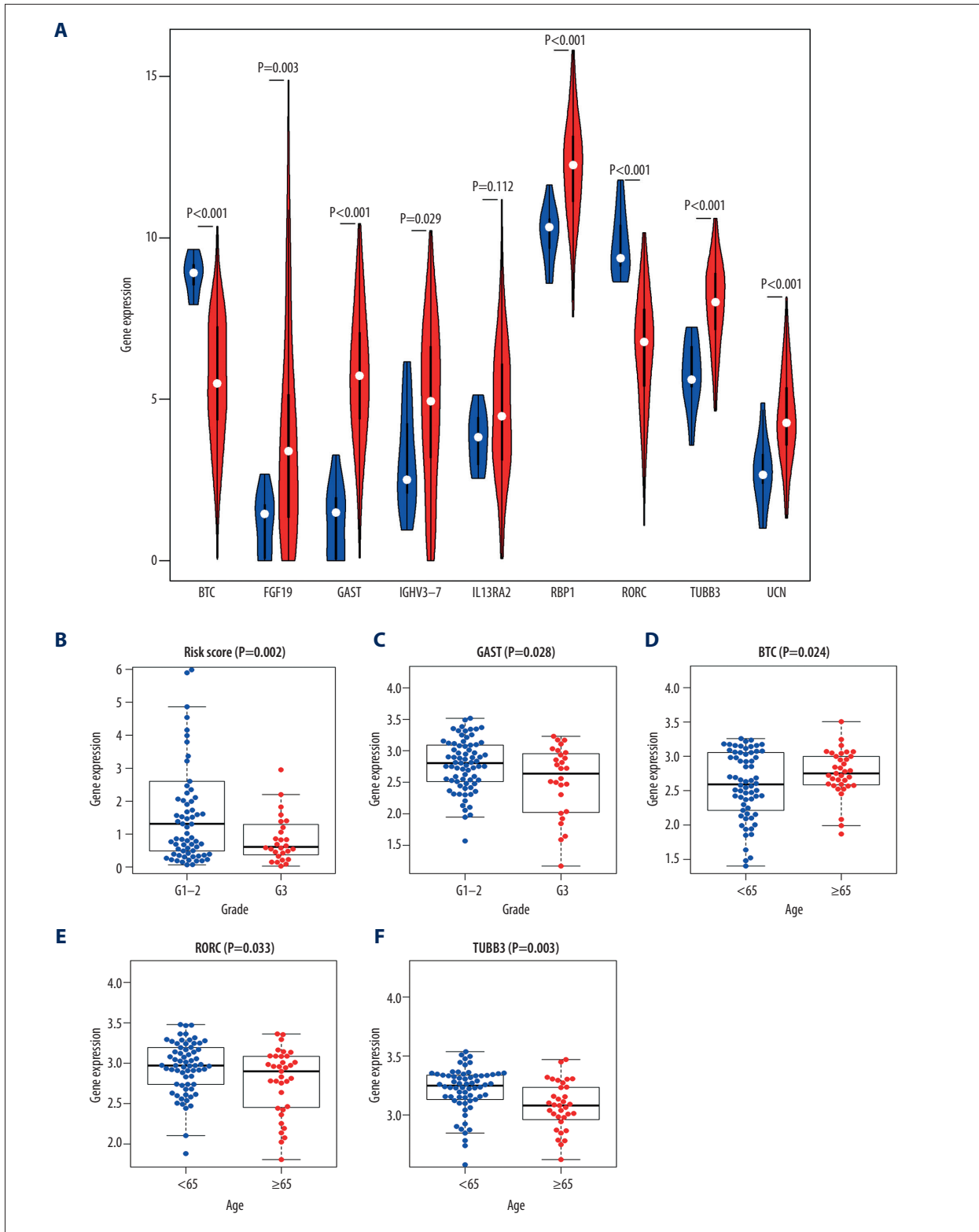


**Figure 9.** Clinical significance of immune-related differentially expressed genes (IRDEGs) signature in laryngeal squamous cell carcinoma (LSCC). **(A)** Violin plot showing the difference in expression levels of 9 IRDEGs between LSCC samples (red violin) and control samples (blue violin), based on Wilcoxon test. **(B–F)** relationship between IRDEGs of signature and clinical parameters. “Grade” means neoplasm histologic grade. Age was in years.

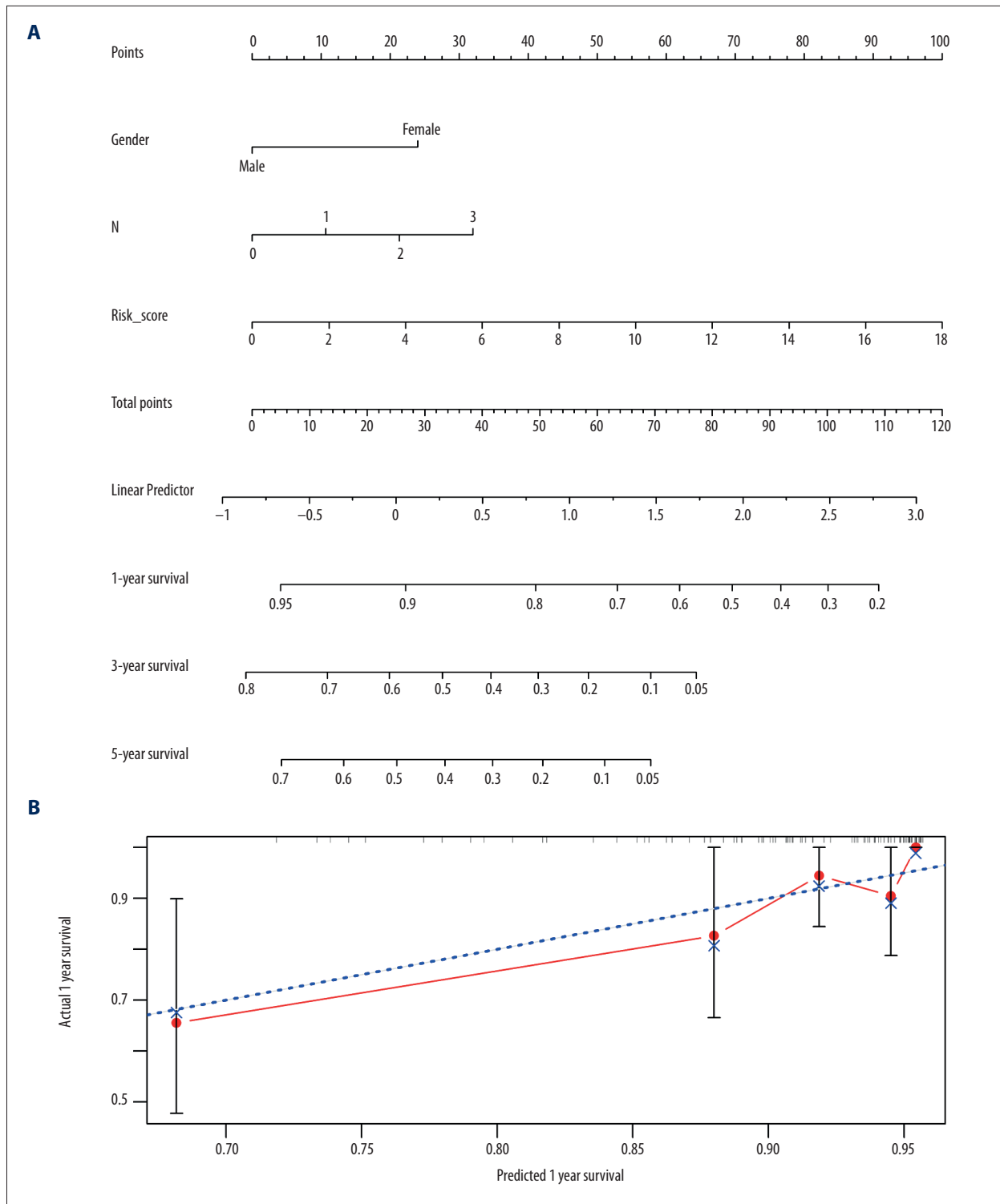


**Figure 10.** Nomogram and corresponding verification. **(A)** Nomogram based on immune-related differentially expressed genes and clinical parameters. **(B)** Calibration curve with a horizontal axis that represents the predicted value of the nomogram and a vertical axis representing the actual survival rate of patients. N, nodes stage.

and down-IRDEGs was the “cytokine-cytokine receptor interaction.” It is worth mentioning that quite a few GO terms and KEGG signaling pathways enriched in IRDEGs were closely related to tumor progression and immune response [48,49]; this, to a certain extent, indicates that IRDEGs may be involved in immune response, and thus, they participate in the occurrence and progression of LSCC. Through PPI analysis, we found that in up-IRDEGs, *KNG1* and *CXCL10* were likely the hub genes in the development of LSCC, and in down-IRDEGs, *ELANE* and *LYZ* were the hub genes. Interestingly, each of these 4 hub genes were considered a potential marker for screening or treating at least 1 cancer [50–53], suggesting that they are essential genes in LSCC. In addition, to explore the upstream regulatory mechanism of IRDEGs, we predicted TRs related to up-IRDEGs and down-IRDEGs and plotted a TR-mediated regulatory network according to the co-expression relationship between TRs and IRDEGs. *SPI1*, *SP140*, and *STAT4* were likely to be key TRs regulating up-IRDEGs; *ZEB1* and *IKZF2* may be the important TRs regulating down-IRDEGs. Although in previous studies, *SPI1* [54] and *STAT4* [55] have been identified as influencing tumors, insight into the regulatory mechanisms of these 5 TRs in LSCC is limited in the literature and more research is needed to verify their role.

To explore new markers that can be used for the screening and treatment of LSCC, we constructed a signature from 9 IRDEGs (*BTC*, *FGF19*, *GAST*, *IGHV3-7*, *IL13RA2*, *RBP1*, *RORC*, *TUBB3*, and *UCN*), and the screening and prognostic effects of it in LSCC were evaluated. In terms of screening, according to the ROC curves, the risk score calculated for the signature proved better at predicting the prognosis of patients with LSCC than any single parameter including age, sex, neoplasm histologic grade, stage, or tumor or node stage, as well as any single IRDEG used to create the signature. Moreover, the risk score also was better for screening and predicting prognosis than any of the recently reported prognostic markers for LSCC, namely, *ALCAM* [39], *ATM* [40], *BCL11A* [41], *BCL-2* [42], *DSG2* [43], *EGFR* [44], *FGFR1* [45], *HOXA13* [46], and *IGF-1R* [47]. In terms of prognosis, not only was the OS rate in the high-risk score group significantly lower than in low-risk score group, but the risk curve showed that there were significantly fewer deaths in patients with lower risk scores. The risk score also proved to be an independent prognostic factor for LSCC in multivariate Cox regression analysis. In summary, the IRDEG signature may be a novel marker for the screening and treatment of LSCC.

All the IRDEGs included in the signature other than *IGHV3-7* have been identified as playing a role in tumors. Among them, *BTC* is considered to promote the development of head and neck squamous cell carcinoma (HNSCC) and has been shown to be a prognostic risk factor in patients with the disease [56]; this was confirmed by our research. We also observed a high level of expression of *FGF19*, which also has been identified in

research about HNSCC [57] and which activates the *ERK* signaling cascade to stimulate the progression of nasopharyngeal carcinoma [58]. Another IRDEG signature gene, *GAST*, may contribute to the progression of gastric cancer at the hormone level [59] through participation in neuroendocrine function. In papillary thyroid carcinoma, with which *IL13RA2* has been associated, the gene may be involved in cell migration by enhancing the epithelial-mesenchymal transition. *RBP1* may be a factor associated with poor prognosis in glioblastoma [31]. *RORC* is thought to trigger proliferation of bladder cancer cells, and this process likely results from its ability to inhibit the *PD-L1/integrin beta-6/signal transducer and activator of transcription 3* signal axis [60]. In patients with esophageal squamous cell carcinoma, those who were *TUBB3*-negative had considerably higher DFS and OS rates than those who were *TUBB3*-positive [30]. *UCN* has a dual effect on liver cancer cell metastasis due to its potential involvement in the regulation of cytosolic phospholipase A2 (*cPLA2*) and calcium-independent phospholipase A2 (*iPLA2*), that is, contributing to cell migration via promoting *cPLA2* expression while preventing cell migration through reducing *iPLA2* expression [61]. It is worth mentioning that, with the exception of *TUBB3* [62] (which contributes to shorter progression-free survival and cancer-specific survival in patients), none of the remaining 8 IRDEGs have been reported in LSCC. This demonstrates the novelty of our work and reveals that further research into these 9 IRDEGs in LSCC is still needed.

To further explore the clinical significance of the IRDEG signature in LSCC, we analyzed the relationship between the signature, clinical parameters, and immune cell infiltration level in patients with LSCC. The results demonstrated that the risk score and the levels of expression of *GAST* were related to the neoplasm histologic grade of LSCC, while the levels of expression of *BTC*, *RORC*, and *TUBB3* were related to the age of patients with LSCC; furthermore, neither the IRDEG signature nor the 9 IRDEGs were relevant to sex, stage, or tumor or nodes stage, but larger samples would be required to verify these observations. At the same time, the risk score based on the IRDEG signature was negatively correlated with the level of B-cell immune infiltration, suggesting that the signature may affect the occurrence and progression of LSCC by affecting the B-cell infiltration level. In short, we found that the clinical significance of the IRDEG signature in LSCC was mainly reflected in the neoplasm histologic grade and the B-cell immune infiltration level.

In this study, although we identified potential molecules involved in LSCC from the perspective of IRGs and established the first IRDEG signature related to the prognosis of the disease, there were several limitations. For example, the sample size was relatively small ( $n=123$ ), and a study with a larger sample would be needed to verify the results. Moreover,



because of the limited sample data, we could not externally verify the IRDEG signature, nor could we identify the relationship between the IRDEG signature and specific treatment methods, such as chemotherapy. Further experimental research is needed to verify the clinical significance and molecular mechanisms of the IRDEG signature in LSCC.

## Conclusions

The IRDEG signature constructed in this study had a strong effect on the screening and prognosis of patients with LSCC and it may be considered an independent prognostic factor for use as a new marker in early screening and treatment of LSCC.

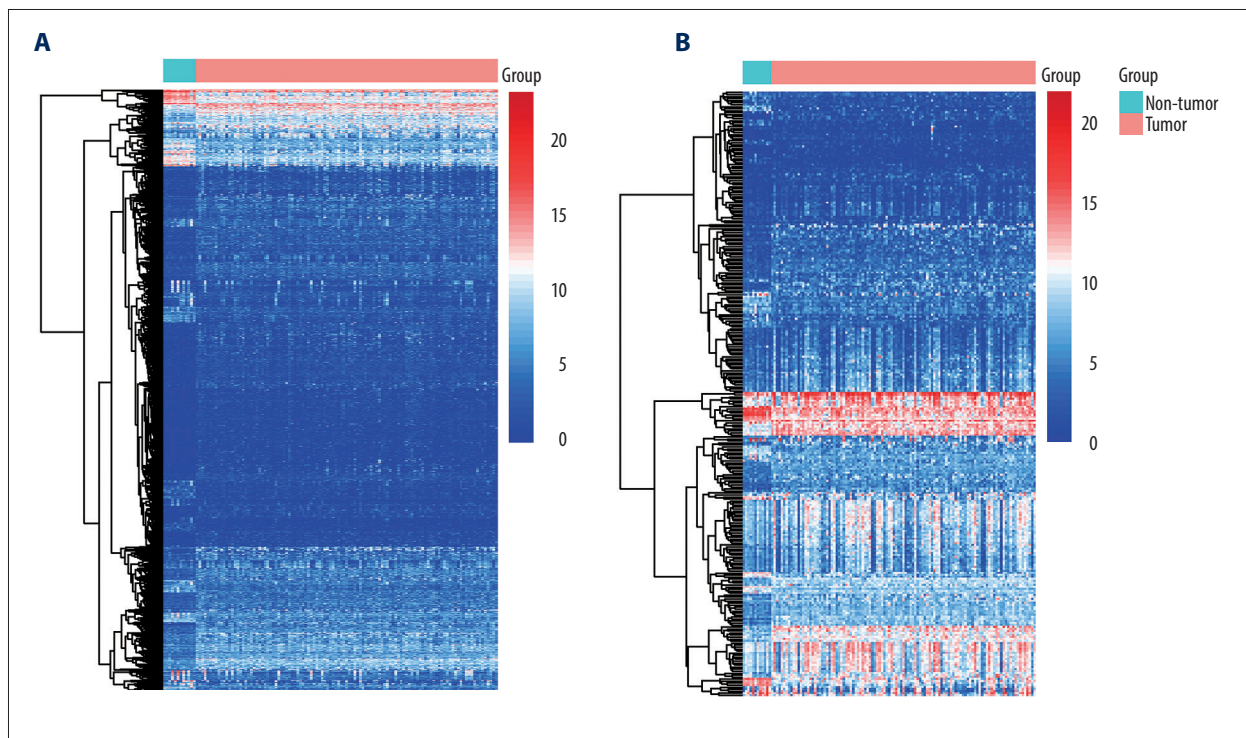
## Supplementary Data

## Acknowledgment

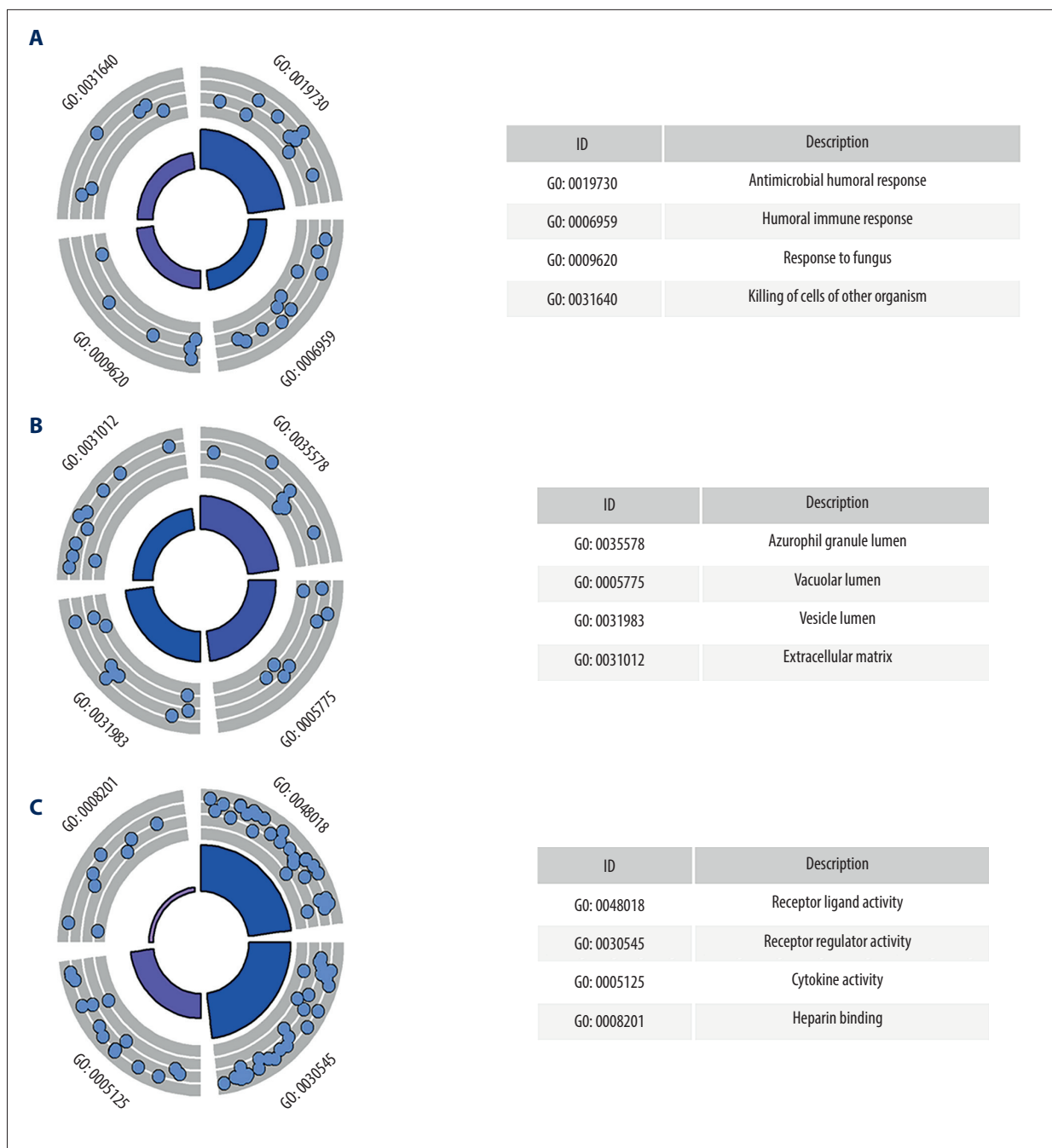
The results of the study are based, in part, upon data generated by The Cancer Genome Atlas Program Research Network: <https://www.cancer.gov/tcga>.

## Conflicts of interest

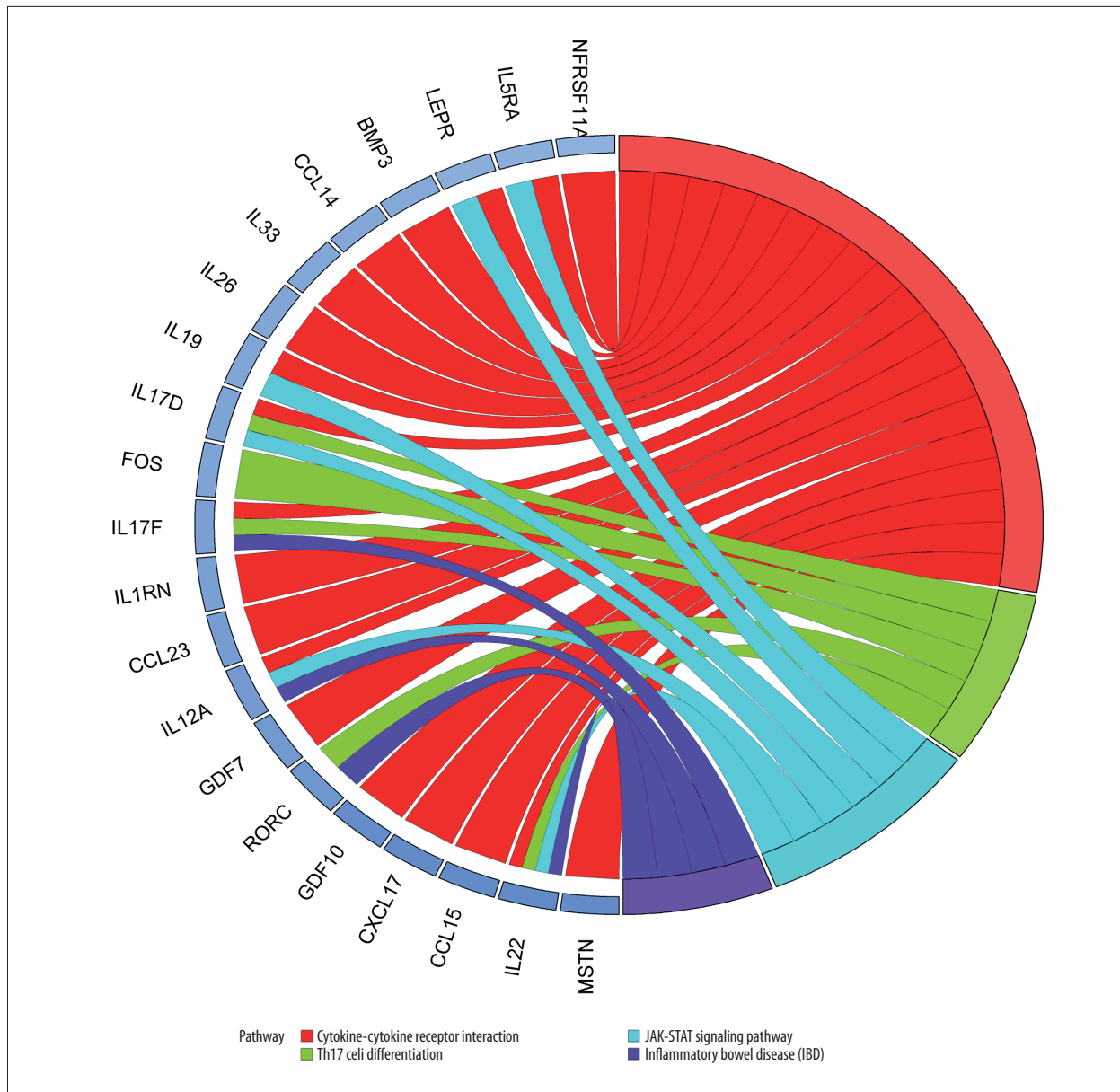
None.



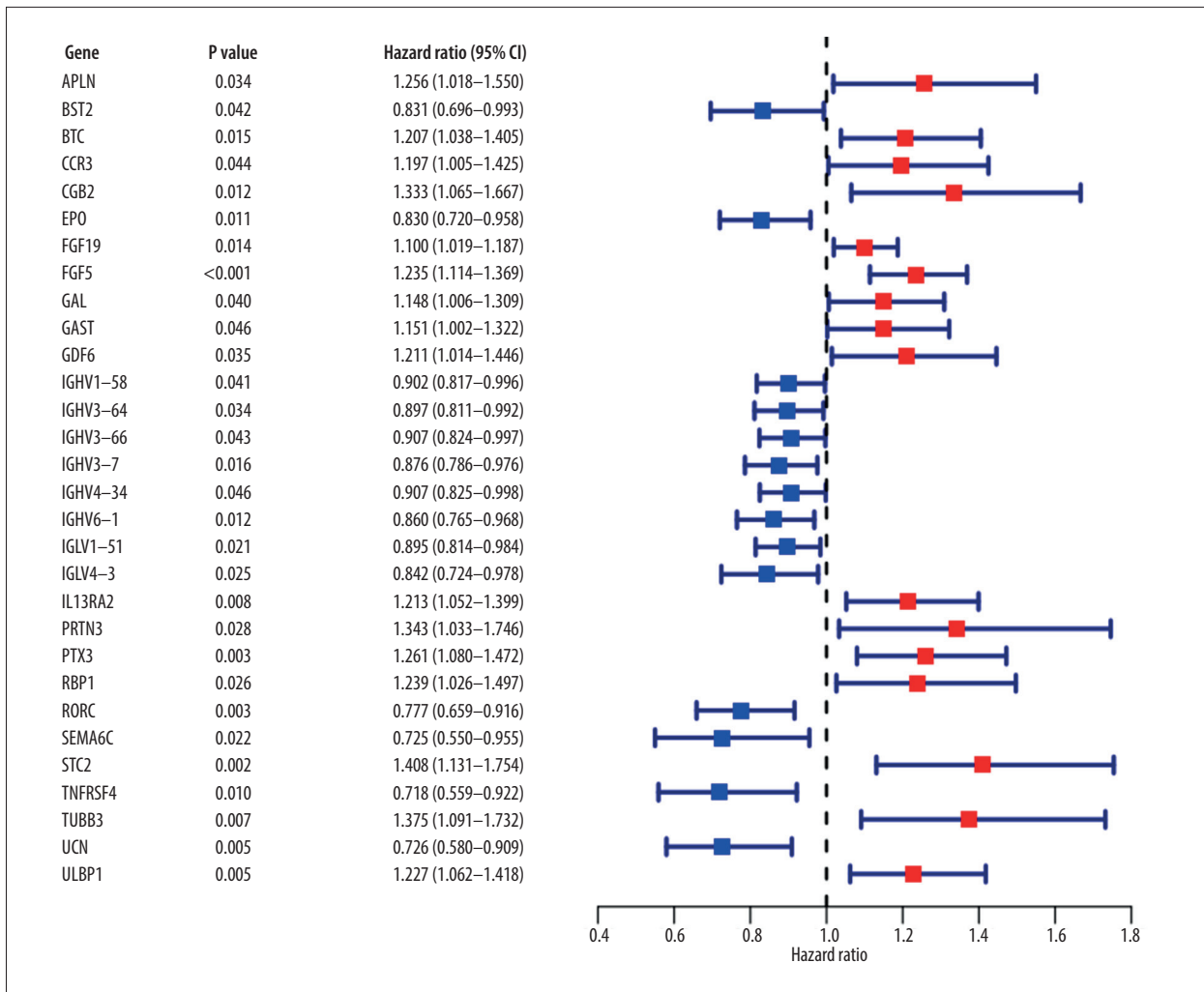
**Supplementary Figure 1.** Differentially expressed genes (DEGs) and immune-related differentially expressed genes (IRDEGs) in laryngeal squamous cell carcinoma (LSCC). Heatmaps demonstrating differentially expressed genes. **(A)** Comparison between LSCC and non-tumor tissues of DEGs. **(B)** Comparison between LSCC and non-tumor tissues of IRDEGs. The depth of color represents the level of gene expression.



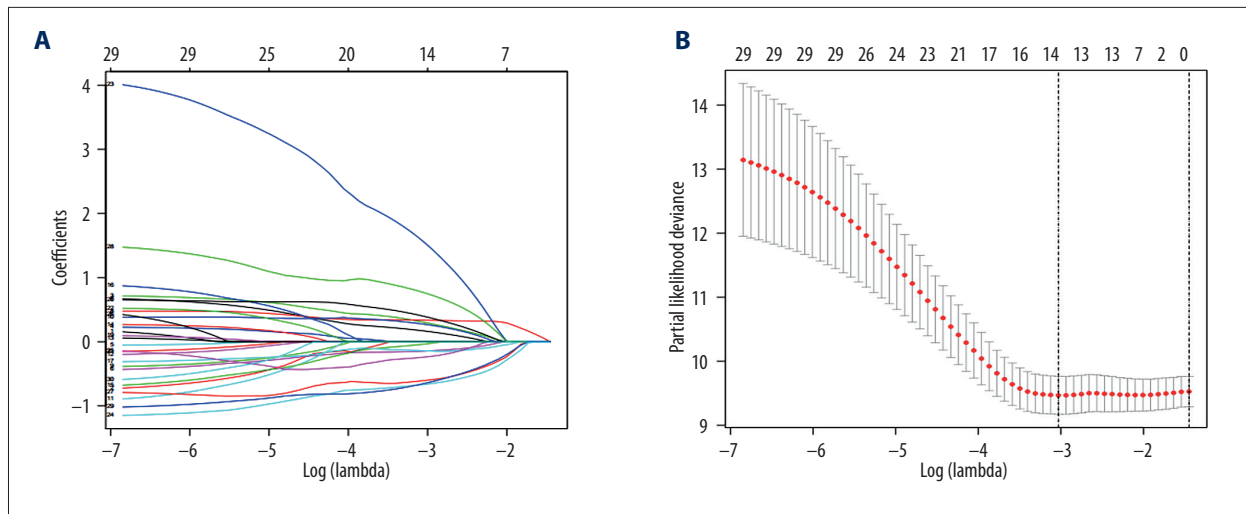
**Supplementary Figure 2.** Gene Ontology (GO) analysis for immune-related downregulated differentially expressed genes. **(A)** Biological process. **(B)** Cellular component. **(C)** Molecular function. The blue nodes in the concentric circles represent genes clustered in specific GO terms. The larger size and darker color of the internal departments represent more significant enrichment of GO term.



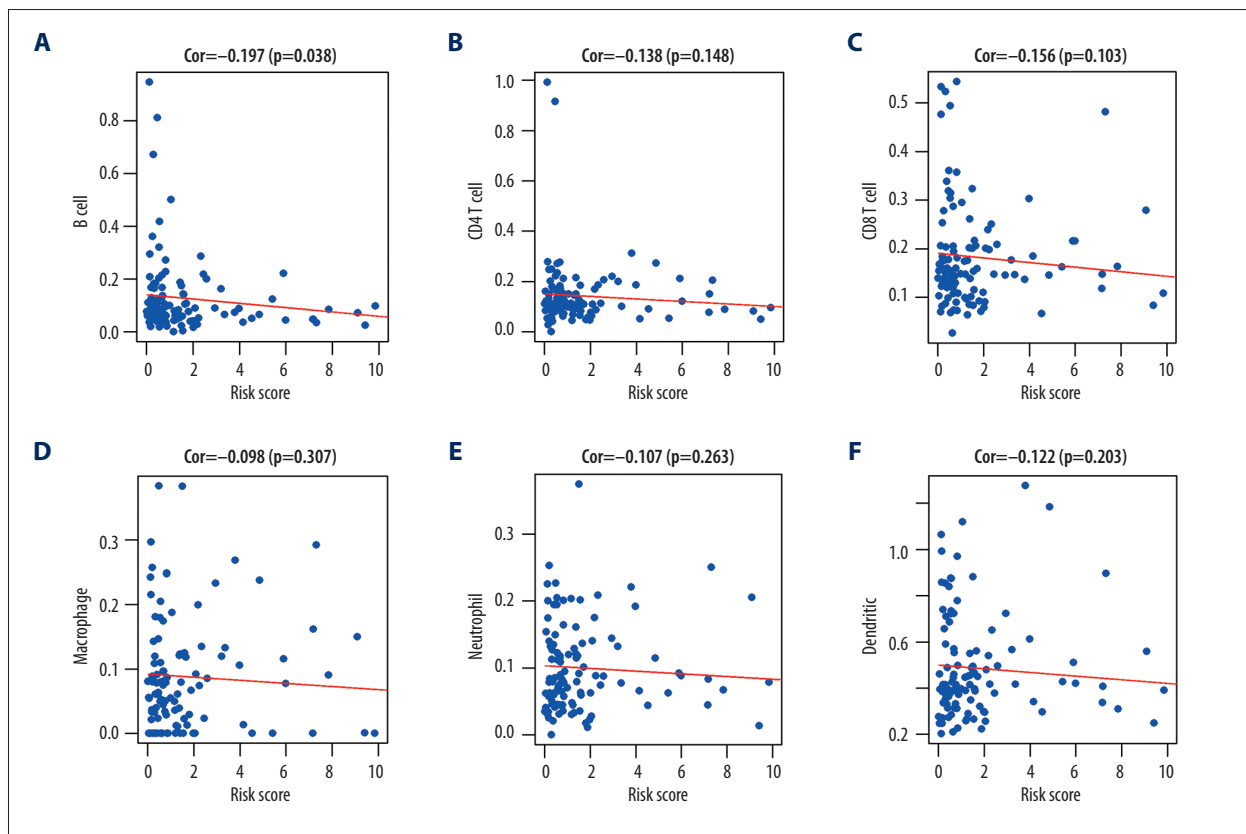
**Supplementary Figure 3.** Kyoto Encyclopedia of Genes and Genomes (KEGG) analysis of immune-related downregulated differentially expressed genes. Different color bands correspond to different KEGG enrichment pathways.



**Supplementary Figure 4.** Forest plot of screening of preliminary candidate immune-related differentially expressed genes (IRDEGs) from 302 IRDEGs.



**Supplementary Figure 5.** Screening of secondary candidate immune-related differentially expressed genes (IRDEGs) for a signature. **(A)** With the continuous increase in lambda, the absolute value of the first 30 preliminary candidate IRDEGs was compressed accordingly. In this process, the absolute value of some relatively unimportant preliminary candidate IRDEGs was compressed to 0. **(B)** Plot of partial likelihood deviance. Each red point corresponds to a lambda value on the lower horizontal axis and a partial likelihood deviance on the vertical axis. The first vertical dashed line on the left corresponds to the highest lambda value, with an average error within 1 standard deviation; from the upper horizontal axis in the figure, this lambda value is based on 14 IRDEGs, which were chosen as secondary candidate IRDEGs.



**Supplementary Figure 6.** (A–F) Relationship between the IRDEG signature and the infiltration level of 6 kinds of immune cells. Cor, correlation coefficient.

**Supplementary Table 1.** Clinical information for 102 patients with laryngeal squamous cell carcinoma.

Sample ID of patients	Age	Gender	Grade	Stage	Tumor stage	Nodes stage	Risk score
TCGA-BA-4076-01	<65	Male	G1-2	Stage III-IV	T3-4	N2-3	1.994791
TCGA-BA-4078-01	≥65	Male	G1-2	Stage III-IV	T1-2	N2-3	7.175697
TCGA-BA-5555-01	<65	Male	G1-2	Stage III-IV	T1-2	N2-3	0.613095
TCGA-BA-6868-01	<65	Male	G1-2	Stage III-IV	T3-4	N2-3	9.846364
TCGA-BA-6869-01	<65	Male	G1-2	Stage III-IV	T3-4	N0-1	1.212306
TCGA-BA-6870-01	<65	Female	G1-2	Stage III-IV	T3-4	N2-3	2.463018
TCGA-BA-A6DA-01	<65	Female	G1-2	Stage III-IV	T3-4	N2-3	0.180343
TCGA-BA-A6DI-01	<65	Male	G1-2	Stage III-IV	T3-4	N0-1	4.540384
TCGA-BB-4217-01	≥65	Male	G3	Stage III-IV	T3-4	N2-3	0.479486
TCGA-CN-4722-01	<65	Female	G1-2	Stage I-II	T1-2	N0-1	0.391675
TCGA-CN-4723-01	≥65	Male	G1-2	Stage III-IV	T3-4	N0-1	1.676743
TCGA-CN-4727-01	<65	Male	G1-2	Stage III-IV	T3-4	N0-1	0.858521
TCGA-CN-4735-01	<65	Male	G3	Stage III-IV	T3-4	N2-3	1.057629
TCGA-CN-4738-01	<65	Male	G1-2	Stage III-IV	T3-4	N0-1	1.380504
TCGA-CN-4739-01	≥65	Male	G1-2	Stage III-IV	T3-4	N0-1	0.209937
TCGA-CN-5355-01	<65	Male	G1-2	Stage III-IV	T3-4	N0-1	1.015923
TCGA-CN-5356-01	<65	Male	G1-2	Stage III-IV	T3-4	N0-1	0.22631
TCGA-CN-5360-01	≥65	Male	G1-2	Stage III-IV	T3-4	N0-1	0.150048
TCGA-CN-5363-01	<65	Male	G3	Stage III-IV	T3-4	N2-3	1.581695
TCGA-CN-6010-01	<65	Male	G1-2	Stage III-IV	T3-4	N0-1	0.485192
TCGA-CN-6012-01	≥65	Male	G1-2	Stage III-IV	T3-4	N0-1	0.698411
TCGA-CN-6021-01	<65	Female	G1-2	Stage III-IV	T3-4	N0-1	7.842248
TCGA-CN-6022-01	<65	Male	G3	Stage III-IV	T3-4	N0-1	2.948932
TCGA-CN-6988-01	<65	Male	G3	Stage III-IV	T3-4	N2-3	0.143416
TCGA-CN-6989-01	<65	Male	G1-2	Stage III-IV	T3-4	N2-3	4.86375
TCGA-CN-6992-01	<65	Male	G1-2	Stage III-IV	T3-4	N0-1	0.676387
TCGA-CN-6997-01	≥65	Male	G3	Stage III-IV	T3-4	N2-3	1.203079
TCGA-CN-A497-01	<65	Male	G1-2	Stage III-IV	T1-2	N2-3	0.070669
TCGA-CN-A49B-01	≥65	Male	G3	Stage III-IV	T3-4	N0-1	2.197291
TCGA-CN-A63T-01	<65	Male	G3	Stage III-IV	T3-4	N2-3	1.399677
TCGA-CN-A63U-01	<65	Male	G3	Stage III-IV	T3-4	N0-1	0.641362
TCGA-CN-A63W-01	<65	Female	G1-2	Stage III-IV	T3-4	N2-3	2.018491
TCGA-CN-A641-01	<65	Male	G1-2	Stage III-IV	T3-4	N2-3	1.561376
TCGA-CN-A6V3-01	<65	Male	G3	Stage III-IV	T3-4	N2-3	0.086898
TCGA-CR-6474-01	<65	Male	G1-2	Stage III-IV	T3-4	N2-3	9.085744

**Supplementary Table 1 continued.** Clinical information for 102 patients with laryngeal squamous cell carcinoma.

Sample ID of patients	Age	Gender	Grade	Stage	Tumor stage	Nodes stage	Risk score
TCGA-CR-7364-01	≥65	Male	G1-2	Stage III-IV	T3-4	N0-1	1.727247
TCGA-CR-7370-01	≥65	Female	G1-2	Stage I-II	T1-2	N0-1	2.24474
TCGA-CR-7371-01	<65	Female	G1-2	Stage III-IV	T3-4	N0-1	3.987309
TCGA-CR-7374-01	≥65	Female	G1-2	Stage I-II	T1-2	N0-1	2.598793
TCGA-CR-7388-01	≥65	Female	G1-2	Stage III-IV	T1-2	N2-3	2.350348
TCGA-CR-7389-01	<65	Male	G1-2	Stage III-IV	T1-2	N0-1	1.464127
TCGA-CR-7398-01	<65	Female	G1-2	Stage I-II	T1-2	N0-1	1.308124
TCGA-CR-7399-01	<65	Female	G3	Stage III-IV	T3-4	N2-3	0.832214
TCGA-CR-7402-01	≥65	Male	G1-2	Stage III-IV	T3-4	N0-1	0.304261
TCGA-CV-5430-01	<65	Male	G3	Stage III-IV	T3-4	N2-3	0.323973
TCGA-CV-5431-01	≥65	Male	G3	Stage III-IV	T3-4	N2-3	0.58173
TCGA-CV-5432-01	≥65	Male	G3	Stage III-IV	T3-4	N0-1	0.455714
TCGA-CV-5434-01	<65	Male	G1-2	Stage III-IV	T3-4	N0-1	0.572978
TCGA-CV-5435-01	<65	Male	G3	Stage III-IV	T3-4	N0-1	0.822588
TCGA-CV-5440-01	<65	Male	G3	Stage III-IV	T3-4	N2-3	0.576644
TCGA-CV-5441-01	<65	Male	G3	Stage III-IV	T3-4	N0-1	0.028728
TCGA-CV-5443-01	<65	Male	G3	Stage III-IV	T3-4	N0-1	0.148582
TCGA-CV-5444-01	<65	Male	G3	Stage III-IV	T3-4	N0-1	0.209379
TCGA-CV-5978-01	<65	Female	G1-2	Stage III-IV	T3-4	N2-3	3.792788
TCGA-CV-6935-01	≥65	Male	G3	Stage III-IV	T3-4	N0-1	1.824833
TCGA-CV-6962-01	≥65	Male	G1-2	Stage III-IV	T3-4	N0-1	9.405468
TCGA-CV-7089-01	≥65	Male	G1-2	Stage III-IV	T3-4	N2-3	0.886302
TCGA-CV-7101-01	≥65	Male	G1-2	Stage I-II	T1-2	N0-1	1.524558
TCGA-CV-7177-01	≥65	Female	G1-2	Stage I-II	T1-2	N0-1	14.47409
TCGA-CV-7242-01	<65	Female	G1-2	Stage III-IV	T3-4	N0-1	0.393045
TCGA-CV-7245-01	<65	Male	G1-2	Stage III-IV	T3-4	N0-1	7.160395
TCGA-CV-7247-01	<65	Male	G1-2	Stage I-II	T1-2	N0-1	1.302915
TCGA-CV-7248-01	<65	Female	G1-2	Stage III-IV	T3-4	N2-3	5.899374
TCGA-CV-7250-01	<65	Male	G1-2	Stage III-IV	T3-4	N0-1	0.765147
TCGA-CV-7261-01	<65	Male	G1-2	Stage III-IV	T3-4	N0-1	0.778688
TCGA-CV-7415-01	<65	Male	G1-2	Stage III-IV	T3-4	N0-1	2.108499
TCGA-CV-7418-01	<65	Male	G1-2	Stage III-IV	T3-4	N0-1	5.986007
TCGA-CV-7421-01	≥65	Male	G1-2	Stage III-IV	T3-4	N0-1	12.39132
TCGA-CV-7422-01	<65	Female	G3	Stage III-IV	T3-4	N0-1	1.383207

**Supplementary Table 1 continued.** Clinical information for 102 patients with laryngeal squamous cell carcinoma.

Sample ID of patients	Age	Gender	Grade	Stage	Tumor stage	Nodes stage	Risk score
TCGA-CV-7424-01	≥65	Male	G1-2	Stage III-IV	T3-4	N2-3	1.60996
TCGA-CV-7430-01	<65	Male	G1-2	Stage III-IV	T3-4	N0-1	16.21789
TCGA-CV-7433-01	<65	Male	G3	Stage III-IV	T3-4	N0-1	7.315585
TCGA-CV-A45W-01	≥65	Male	G1-2	Stage III-IV	T3-4	N0-1	0.269141
TCGA-CV-A45Y-01	<65	Male	G3	Stage III-IV	T3-4	N0-1	0.689461
TCGA-CV-A45Z-01	≥65	Male	G3	Stage I-II	T1-2	N0-1	0.854492
TCGA-CV-A460-01	≥65	Male	G3	Stage III-IV	T3-4	N2-3	0.546034
TCGA-CV-A461-01	≥65	Male	G1-2	Stage III-IV	T3-4	N0-1	0.546608
TCGA-CV-A6K1-01	≥65	Male	G1-2	Stage III-IV	T3-4	N0-1	0.360293
TCGA-D6-6517-01	<65	Male	G1-2	Stage III-IV	T3-4	N0-1	0.68767
TCGA-D6-6824-01	<65	Male	G1-2	Stage III-IV	T3-4	N0-1	0.495199
TCGA-D6-6826-01	<65	Female	G1-2	Stage III-IV	T3-4	N2-3	1.514392
TCGA-D6-8568-01	<65	Male	G1-2	Stage I-II	T1-2	N0-1	0.417747
TCGA-D6-A6EK-01	≥65	Male	G1-2	Stage III-IV	T3-4	N0-1	0.189092
TCGA-D6-A6EQ-01	<65	Male	G3	Stage III-IV	T3-4	N0-1	0.545436
TCGA-D6-A6ES-01	<65	Male	G1-2	Stage III-IV	T3-4	N0-1	0.191914
TCGA-D6-A74Q-01	≥65	Male	G3	Stage III-IV	T3-4	N0-1	0.22864
TCGA-DQ-5629-01	<65	Male	G1-2	Stage III-IV	T3-4	N2-3	2.062312
TCGA-F7-7848-01	<65	Male	G1-2	Stage III-IV	T3-4	N0-1	0.690225
TCGA-F7-8298-01	<65	Male	G1-2	Stage I-II	T1-2	N0-1	0.30976
TCGA-KU-A66S-01	≥65	Female	G1-2	Stage III-IV	T1-2	N0-1	4.15964
TCGA-QK-A8Z8-01	<65	Female	G1-2	Stage III-IV	T3-4	N0-1	0.330232
TCGA-QK-A8ZB-01	v65	Male	G1-2	Stage III-IV	T3-4	N0-1	1.588431
TCGA-QK-AA3J-01	≥65	Male	G3	Stage I-II	T1-2	N0-1	0.419213
TCGA-T3-A92M-01	<65	Male	G1-2	Stage III-IV	T3-4	N2-3	3.215592
TCGA-UF-A718-01	<65	Male	G1-2	Stage III-IV	T3-4	N0-1	0.79612
TCGA-UF-A71D-01	<65	Female	G1-2	Stage III-IV	T3-4	N0-1	0.063101
TCGA-UF-A7J9-01	≥65	Male	G1-2	Stage III-IV	T3-4	N0-1	3.368041
TCGA-UF-A7JF-01	≥65	Male	G1-2	Stage III-IV	T3-4	N2-3	0.350744
TCGA-UF-A7JH-01	<65	Male	G1-2	Stage III-IV	T3-4	N0-1	0.220921
TCGA-UF-A7JJ-01	≥65	Male	G1-2	Stage III-IV	T3-4	N0-1	0.834466
TCGA-UF-A7JK-01	<65	Male	G1-2	Stage III-IV	T3-4	N0-1	1.902253

Grade – neoplasm histologic grade.



## References:

1. Gamez ME, Blakaj A, Zoller W et al: Emerging concepts and novel strategies in radiation therapy for laryngeal cancer management. *Cancers (Basel)*, 2020; 12(6): 1651
2. Elicin O, Giger R: Comparison of current surgical and non-surgical treatment strategies for early and locally advanced stage glottic laryngeal cancer and their outcome. *Cancers (Basel)*, 2020; 12(3): 732
3. Wang H, Qian J, Xia X et al: Long non-coding RNA OIP5-AS1 serves as an oncogene in laryngeal squamous cell carcinoma by regulating miR-204-5p/ZEB1 axis. *Naunyn Schmiedebergs Arch Pharmacol*, 2020 [Online ahead of print]
4. Yang T, Li S, Liu J et al: Long non-coding RNA KRT16P2/miR-1294/EGFR axis regulates laryngeal squamous cell carcinoma cell aggressiveness. *Am J Transl Res*, 2020; 12(6): 2939–55
5. Guo Y, Huang Q, Zheng J et al: Diagnostic role of dysregulated circular RNA hsa\_circ\_0036722 in laryngeal squamous cell carcinoma. *Onco Targets Ther*, 2020; 13: 5709–19
6. Tang X-Z, Zhou X-G, Zhang X-G et al: The clinical significance of Interleukin 24 and its potential molecular mechanism in laryngeal squamous cell carcinoma. *Cancer Biomark*, 2020; 29(1): 111–24
7. Bray F, Ferlay J, Soerjomataram I et al: Global cancer statistics 2018: GLOBOCAN estimates of incidence and mortality worldwide for 36 cancers in 185 countries. *Cancer J Clin*, 2018; 68(6): 394–424
8. Dietz A, Wichmann G, Kuhnt T et al: Induction chemotherapy (IC) followed by radiotherapy (RT) versus cetuximab plus IC and RT in advanced laryngeal/hypopharyngeal cancer resectable only by total laryngectomy-final results of the larynx organ preservation trial DeLOS-II. *Ann Oncol*, 2018; 29(10): 2105–14
9. Steuer CE, El-Deiry M, Parks JR et al: An update on larynx cancer. *Cancer J Clin*, 2017; 67(1): 31–50
10. Pedregal-Mallo D, Sánchez Canteli M, López F et al: Oncological and functional outcomes of transoral laser surgery for laryngeal carcinoma. *Eur Arch Otorhinolaryngol*, 2018; 275(8): 2071–77
11. Giotakis AI, Pototschnig C: Use of erbium laser in the treatment of persistent post-radiotherapy laryngeal edema: A case report and review of the literature. *World J Surg Oncol*, 2018; 16(1): 176.
12. Dietz A, Wiegand S, Kuhnt T et al: Laryngeal preservation approaches: Considerations for new selection criteria based on the DeLOS-II Trial. *Front Oncol*, 2019; 9: 625
13. Menach OP, Patel A, Oburra HO: Demography and histologic pattern of laryngeal squamous cell carcinoma in Kenya. *Int J Otolaryngol*, 2014; 2014: 507189
14. de Bree R: The current indications for non-surgical treatment of hypopharyngeal cancer. *Adv Otorhinolaryngol*, 2019; 83: 76–89
15. Fulcher CD, Haigentz M, Ow TJ: AHSN Series: Do you know your guidelines? Principles of treatment for locally advanced or unresectable head and neck squamous cell carcinoma. *Head Neck*, 2018; 40(4): 676–86
16. Mannelli G, Lazio MS, Luparello P et al: Conservative treatment for advanced T3-T4 laryngeal cancer: Meta-analysis of key oncological outcomes. *Eur Arch Otorhinolaryngol*, 2018; 275(1): 27–38
17. Nocini R, Molteni G, Mattiuzzi C et al: Updates on larynx cancer epidemiology. *Chin J Cancer Res*, 2020; 32(1): 18–25
18. Praud D, Rota M, Rehm J et al: Cancer incidence and mortality attributable to alcohol consumption. *Int J Cancer*, 2016; 138(6): 1380–87
19. Ahmad Kiadaliri A, Jarl J, Gavrilidis G et al: Alcohol drinking cessation and the risk of laryngeal and pharyngeal cancers: A systematic review and meta-analysis. *PLoS One*, 2013; 8(3): e58158
20. Kawakita D, Matsuo K: Alcohol and head and neck cancer. *Cancer Metastasis Rev*, 2017; 36(3): 425–34
21. Kang D-M, Kim J-E, Kim Y-K et al: Occupational burden of asbestos-related diseases in Korea, 1998–2013: Asbestosis, mesothelioma, lung cancer, laryngeal cancer, and ovarian cancer. *J Korean Med Sci*, 2018; 33(35): e226
22. Yang D, Shi Y, Tang Y et al: Effect of HPV Infection on the occurrence and development of laryngeal cancer: A review. *J Cancer*, 2019; 10(19): 4455–62
23. Wang H-T, Tong X, Zhang Z-X et al: MYC1 represses apoptosis of laryngeal cancerous cells through the MAX/miR-181a/NPM1 pathway. *FEBS J*, 2019; 286(19): 3892–908
24. Dogantemur S, Ozdemir S, Uguz A et al: Assessment of HPV 16, HPV 18, p16 expression in advanced stage laryngeal cancer patients and prognostic significance. *Braz J Otorhinolaryngol*, 2020; 86(3): 351–57
25. Shen N, Duan XH, Wang XL et al: Effect of NLK on the proliferation and invasion of laryngeal carcinoma cells by regulating CDCP1. *Eur Rev Med Pharmacol Sci*, 2019; 23(14): 6226–33
26. Tang X, Sun Y, Wan G et al: Knockdown of YAP inhibits growth in Hep-2 laryngeal cancer cells via epithelial-mesenchymal transition and the Wnt/ $\beta$ -catenin pathway. *BMC Cancer*, 2019; 19(1): 654
27. Yang J, Zhou L, Zhang Y et al: DIAPH1 is upregulated and inhibits cell apoptosis through ATR/p53/Caspase-3 signaling pathway in laryngeal squamous cell carcinoma. *Dis Markers*, 2019; 2019: 6716472
28. Zhu X, Zhu R: Curcumin suppresses the progression of laryngeal squamous cell carcinoma through the upregulation of miR-145 and inhibition of the PI3K/Akt/mTOR pathway. *Onco Targets Ther*, 2018; 11: 3521–31
29. Zhao X, Xu F, Dominguez NP et al: FGFR4 provides the conduit to facilitate FGF19 signaling in breast cancer progression. *Mol Carcinog*, 2018; 57(11): 1616–25
30. Gong L, Mao W, Chen Q et al: Analysis of SPARC and TUBB3 as predictors for prognosis in esophageal squamous cell carcinoma receiving nab-paclitaxel plus cisplatin neoadjuvant chemotherapy: A prospective study. *Cancer Chemother Pharmacol*, 2019; 83(4): 639–47
31. Erhart F, Hackl M, Hahne H et al: Combined proteomics/miRNomics of dendritic cell immunotherapy-treated glioblastoma patients as a screening for survival-associated factors. *NPJ Vaccines*, 2020; 5: 5
32. Birtalan E, Danos K, Gurbi B et al: Expression of PD-L1 on immune cells shows better prognosis in laryngeal, oropharyngeal, and hypopharyngeal cancer. *Appl Immunohistochem Mol Morphol*, 2018; 26(7): e79–85
33. Zhang C, Guan Z, Peng J: [The correlation between stanniocalcin 2 expression and prognosis in laryngeal squamous cell cancer]. *Lin Chung Er Bi Yan Hou Tou Jing Wai Ke Za Zhi*, 2015; 29(2): 102–7 [in Chinese]
34. Robinson MD, McCarthy DJ, Smyth GK: edgeR: A Bioconductor package for differential expression analysis of digital gene expression data. *Bioinformatics*, 2010; 26(1): 139–40
35. Yu G, Wang L-G, Han Y et al: clusterProfiler: An R package for comparing biological themes among gene clusters. *OMICS*, 2012; 16(5): 284–87
36. Qin Q, Fan J, Zheng R et al: Lisa: Inferring transcriptional regulators through integrative modeling of public chromatin accessibility and ChIP-seq data. *Genome Biol*, 2020; 21(1): 32
37. Engebretsen S, Bohlin J: Statistical predictions with glmnet. *Clin Epigenetics*, 2019; 11(1): 123
38. Heagerty PJ, Zheng Y: Survival model predictive accuracy and ROC curves. *Biometrics*, 2005; 61(1): 92–105
39. Nicolau-Neto P, de Souza-Santos PT, Severo Ramundo M et al: Transcriptome analysis identifies ALCAM overexpression as a prognosis biomarker in laryngeal squamous cell carcinoma. *Cancers (Basel)*, 2020; 12(2): 470
40. Bruine de Bruin L, Schuurung E, de Bock GH et al: High pATM is associated with poor local control in supraglottic cancer treated with radiotherapy. *Laryngoscope*, 2020; 130(8): 1954–60
41. Zhou J, Zhou L, Zhang D et al: BCL11A promotes the progression of laryngeal squamous cell carcinoma. *Front Oncol*, 2020; 10: 375
42. Lovato A, Franz L, Carraro V et al: Maspin expression and anti-apoptotic pathway regulation by bcl2 in laryngeal cancer. *Ann Diagn Pathol*, 2020; 45: 151471
43. Cury SS, Lapa RML, de Mello JBH et al: Increased DSG2 plasmatic levels identified by transcriptomic-based secretome analysis is a potential prognostic biomarker in laryngeal carcinoma. *Oral Oncol*, 2020; 103: 104592
44. Leesutipornchai T, Ratchataswan T, Vivatvakin S et al: EGFR cut-off point for prognostic impact in laryngeal squamous cell carcinoma. *Acta Otolaryngol*, 2020; 140(7): 610–14
45. Klobučar M, Visentin S, Jakovčević A et al: Expression of polysialic acid in primary laryngeal squamous cell carcinoma. *Life Sci*, 2017; 173: 73–79
46. Li J, Ye M, Zhou C: Expression profile and prognostic values of family members in laryngeal squamous cell cancer. *Front Oncol*, 2020; 10: 368
47. Ben Elhadj M, Goucha A, Fourati A et al: The prognostic significance of IGF-1R and the predictive risk value of circulating IGF-1 in Tunisian patients with laryngeal carcinoma. *Cancer Invest*, 2020; 38(5): 289–99

48. Szczerba BM, Castro-Giner F, Vetter M et al: Neutrophils escort circulating tumour cells to enable cell cycle progression. *Nature*, 2019; 566(7745): 553–57
49. Macor P, Capolla S, Tedesco F: Complement as a biological tool to control tumor growth. *Front Immunol*, 2018; 9: 2203
50. Xu J, Fang J, Cheng Z et al: Overexpression of the Kininogen-1 inhibits proliferation and induces apoptosis of glioma cells. *J Exp Clin Cancer Res*, 2018; 37(1): 180
51. Karin N: Chemokines and cancer: New immune checkpoints for cancer therapy. *Curr Opin Immunol*, 2018; 51: 140–45
52. Sarvestani SK, Signs SA, Lefebvre V et al: Cancer-predicting transcriptomic and epigenetic signatures revealed for ulcerative colitis in patient-derived epithelial organoids. *Oncotarget*, 2018; 9(47): 28717–30
53. Wei Z, Wu B, Wang L et al: A large-scale transcriptome analysis identified ELANE and PRTN3 as novel methylation prognostic signatures for clear cell renal cell carcinoma. *J Cell Physiol*, 2020; 235(3): 2582–89
54. Luo D, Ge W: MeCP2 promotes colorectal cancer metastasis by modulating ZEB1 transcription. *Cancers (Basel)*, 2020; 12(3): 758
55. Zhou Y, Zhong J-H, Gong F-S et al: MiR-141-3p suppresses gastric cancer induced transition of normal fibroblast and BMSC to cancer-associated fibroblasts via targeting STAT4. *Exp Mol Pathol*, 2019; 107: 85–94
56. Gao J, Ulekleiv CH, Halstensen TS: Epidermal growth factor (EGF) receptor-ligand based molecular staging predicts prognosis in head and neck squamous cell carcinoma partly due to deregulated EGF-induced amphiregulin expression. *J Exp Clin Cancer Res*, 2016; 35(1): 151
57. Gao L, Lang L, Zhao X et al: FGF19 amplification reveals an oncogenic dependency upon autocrine FGF19/FGFR4 signaling in head and neck squamous cell carcinoma. *Oncogene*, 2019; 38(13): 2394–404
58. Shi S, Zhang Q, Xia Y et al: Mesenchymal stem cell-derived exosomes facilitate nasopharyngeal carcinoma progression. *Am J Cancer Res*, 2016; 6(2): 459–72
59. Speck O, Tang W, Morgan DR et al: Three molecular subtypes of gastric adenocarcinoma have distinct histochemical features reflecting Epstein-Barr virus infection status and neuroendocrine differentiation. *Appl Immunohistochem Mol Morphol*, 2015; 23(9): 633–45
60. Cao D, Qi Z, Pang Y et al: Retinoic acid-related orphan receptor c regulates proliferation, glycolysis, and chemoresistance via the PD-L1/ITGB6/STAT3 signaling axis in bladder cancer. *Cancer Res*, 2019; 79(10): 2604–18
61. Zhu C, Sun Z, Li C et al: Urocortin affects migration of hepatic cancer cell lines via differential regulation of cPLA2 and iPLA2. *Cell Signal*, 2014; 26(5): 1125–34
62. Koh Y, Kim TM, Jeon YK et al: Class III beta-tubulin, but not ERCC1, is a strong predictive and prognostic marker in locally advanced head and neck squamous cell carcinoma. *Ann Oncol*, 2009; 20(8): 1414–19